

The multiplicative deformation split for shells with application to growth, chemical swelling, thermoelasticity, viscoelasticity and elastoplasticity

Roger A. Sauer^{*,1}, Reza Ghaffari^{*} and Anurag Gupta[†]

^{*}*Aachen Institute for Advanced Study in Computational Engineering Science (AICES),
RWTH Aachen University, Templergraben 55, 52056 Aachen, Germany*

[†]*Department of Mechanical Engineering, Indian Institute of Technology Kanpur, UP 208016, India*

Published² in *Int. J. Solids Struc.*, DOI: [10.1016/j.ijsolstr.2019.06.002](https://doi.org/10.1016/j.ijsolstr.2019.06.002)

Submitted on 3. December 2018, Revised on 20. May 2019, Accepted on 4. June 2019

Abstract

This work presents a general unified theory for coupled nonlinear elastic and inelastic deformations of curved thin shells. The coupling is based on a multiplicative decomposition of the surface deformation gradient. The kinematics of this decomposition is examined in detail. In particular, the dependency of various kinematical quantities, such as area change and curvature, on the elastic and inelastic strains is discussed. This is essential for the development of general constitutive models. In order to fully explore the coupling between elastic and different inelastic deformations, the surface balance laws for mass, momentum, energy and entropy are examined in the context of the multiplicative decomposition. Based on the second law of thermodynamics, the general constitutive relations are then derived. Two cases are considered: Independent inelastic strains, and inelastic strains that are functions of temperature and concentration. The constitutive relations are illustrated by several nonlinear examples on growth, chemical swelling, thermoelasticity, viscoelasticity and elastoplasticity of shells. The formulation is fully expressed in curvilinear coordinates leading to compact and elegant expressions for the kinematics, balance laws and constitutive relations.

Keywords: Curvilinear coordinates, inelastic shells, irreversible thermodynamics, multiplicative decomposition, nonlinear shell theory, Kirchhoff-Love kinematics

1 Introduction

Many problems in science and technology are characterized by different, competing deformation types. Apart from elastic deformations, which are studied predominantly in solid mechanics, deformations can also arise from growth, swelling, thermal expansion, viscosity, plasticity and electro-magnetical fields. The decomposition of these deformations is essential for the proper modeling and understanding of coupled problems. In thermoelasticity, for instance, mechanical stresses do not arise from thermal deformations, but from the elastic deformations countering those. In the general framework of large deformations, the decomposition of deformations is based on the multiplicative split of the deformation gradient. While the topic has been studied extensively for three-dimensional continua, there are much fewer works studying the

¹corresponding author, email: sauer@aices.rwth-aachen.de

²This pdf is the personal version of an article whose final publication is available at www.sciencedirect.com

multiplicative split for curved surfaces. In particular, a general shell theory that unifies different deformation types is currently lacking and therefore addressed here.

The origins of the multiplicative decomposition of the deformation gradient can be traced back to [Flory \(1950\)](#), who used a 1D version of it to decompose elastic and inelastic stretches during swelling, [Eckart \(1948\)](#) and [Kondo \(1949\)](#), who introduced the notion of a locally relaxed (stress-free) intermediate configuration that can be globally incompatible, and [Bilby et al. \(1957\)](#) and [Kröner \(1959\)](#), who formalized the multiplicative decomposition for plasticity. Recent discussion on the origin, mathematical nature and application of the multiplicative decomposition has been provided by [Lubarda \(2004\)](#), [Gupta et al. \(2007\)](#) and [Reina et al. \(2018\)](#). Following its introduction for swelling and plasticity, the multiplicative decomposition has been extended to thermoelasticity ([Stojanović et al., 1964](#)), viscoelasticity ([Sidoroff, 1974](#)) and growth ([Kondaurov and Nikitin, 1987](#); [Takamizawa and Hayashi, 1987](#)). Subsequently, a vast literature body has appeared on the topic. Most of it deals with 3D continua or shell formulations derived from those using the *degenerate solid* framework ([Ahmad et al., 1970](#); [Parisich, 1978](#)). These cases are based on a deformation decomposition in 3D – usually in the context of Cartesian coordinate systems. Instead of this, we are concerned here with a decomposition of the surface deformation in the general framework of curvilinear coordinates. Therefore we restrict the following survey to general shell structures based on such surface formulations.

Growth and swelling of shells: The first general surface formulations using a multiplicative decomposition to couple mechanical deformation and growth seem to be the works by [Dervaux et al. \(2009\)](#) and [Wang et al. \(2018\)](#) on plates, [Rausch and Kuhl \(2014\)](#) on membranes, [Vetter et al. \(2013, 2014\)](#) on Kirchhoff-Love shells, and [Lychev \(2014\)](#) on Reissner-Mindlin shells. Similar approaches have also been considered by [Papastavrou et al. \(2013\)](#) to model surface growth of bulk materials and [Swain and Gupta \(2018\)](#) to model interface growth. A general surface formulation coupling mechanical deformation and swelling of membranes and shells seems to have appeared only recently by the work of [Lucantonio et al. \(2017\)](#).

Viscoelasticity of shells: The work by [Neff \(2005\)](#) seems to be the first general surface model for viscoelastic shells and membranes that is using a multiplicative decomposition of the deformation. All subsequent works seem to have resorted back to additive decompositions. Examples are the works by [Lubarda \(2011\)](#) on erythrocyte membranes, [Li \(2012\)](#) on the derivation of shell formulations from 3D viscoelasticity, [Altenbach and Eremeyev \(2015\)](#) on micropolar shells and [Dörr et al. \(2017\)](#) on fiber reinforced composite shells.

Elastoplasticity of shells: The research on general elastoplastic shells goes back to the works by [Green et al. \(1968\)](#), [Sawczuk \(1982\)](#), [Başar and Weichert \(1991\)](#) and [Simo and Kennedy \(1992\)](#). They follow however an additive decomposition of the strain. The work by [Simo and Kennedy \(1992\)](#), seems to be the first FE model that is directly based on a surface formulation instead of considering the thickness integration of 3D continua, as has been done by many others, e.g. see [Stumpf and Schieck \(1994\)](#), [Miehe \(1998\)](#), [Betsch and Stein \(1999\)](#), [Eberlein and Wriggers \(1999\)](#) and recently [Steigmann \(2015\)](#) and [Ambati et al. \(2018\)](#). This property clearly distinguishes these works from the approach taken here: Instead of integrating 3D continua, here the entire theory, including the multiplicative decomposition, is directly based on a surface formulation. The recent surface formulations by [Dujc and Brank \(2012\)](#) and [Roychowdhury and Gupta \(2018\)](#), on the other hand, are based again on an additive split, although the existence of a multiplicative split of the surface deformation gradient has been alluded to in the latter work.

Thermomechanics of shells: General surface formulations for thermomechanical shells have been developed by [Green and Naghdi \(1979\)](#), [Reddy and Chin \(1998\)](#) and recently [Kar and Panda \(2016\)](#). However, none of these formulations is based on a multiplicative decomposition.

Instead, a general surface formulation for thermomechanical shells based on a multiplicative decomposition seems to be still lacking.

The survey shows that even though many works have appeared on coupled elastic and inelastic deformations for shells, only few use a general surface formulation in the general framework of curvilinear coordinates, and none seem to start from a multiplicative decomposition of the surface deformation gradient. Instead they either start from an additive decomposition or they are based on thickness integration of the classical multiplicative decomposition.

The use of a curvilinear coordinate description allows for a very general treatment of shell geometry and deformation. Also it allows for a direct finite element (FE) formulation that avoids the overhead of a transformation to a Cartesian formulation as is classically used. Shell FE formulations tend to be much more efficient than classical 3D FE formulations, since no thickness discretization is needed. Instead, simplifying assumptions are used for the thickness behavior. The most efficient shell formulation is based on Kirchhoff-Love kinematics, which assumes that cross-sections remain planar and normal to the mid-plane during deformation. Further, a normal thickness stress is usually neglected. These assumptions are suitable for thin shells, whose planar dimensions are at least one order of magnitude larger than the thickness. Following the works by Prigogine (1961), de Groot and Mazur (1984), Naghdi (1972) and Steigmann (1999) on irreversible thermodynamics and nonlinear Kirchhoff-Love shell theory, Sauer and Duong (2017) and Sahu et al. (2017) recently developed a new multiphysical shell theory that is suitable for both solid and liquid shells. Based on this theory, new finite element formulations have been proposed for engineering shells (Duong et al., 2017), layered shells (Roohbakhshan and Sauer, 2016), biological shells (Roohbakhshan and Sauer, 2017), graphene (Ghaffari et al., 2017), lipid bilayers (Sauer et al., 2017), inverse analysis (Vu-Bac et al., 2018), phase transformations (Zimmermann et al., 2019) and surfactants (Roohbakhshan and Sauer, 2019). However, all of these works are restricted to elastic deformations.

The restrictions in the current literature mentioned above motivates the development of a general thin shell formulation for coupled deformations. Such a formulation should be based on a multiplicative split, in order to handle large deformations, use curvilinear coordinates, in order to handle general surface geometries, and account for the laws of irreversible thermodynamics, in order to capture the full scope of coupling. Compared to existing formulations, the formulation proposed here has several novelties:

- It provides a unified shell theory for coupled nonlinear elastic and inelastic deformations.
- It is based on the multiplicative decomposition of the surface deformation gradient.
- It accounts for growth, swelling, viscosity, plasticity and thermal deformations.
- It is fully formulated in the general and compact framework of curvilinear coordinates.
- It explores the coupling in the kinematic relations and local balance laws.
- It is illustrated by several constitutive examples derived from the second law of thermodynamics.

It is also shown that the multiplicative split on the surface deformation gradient generally leads to an additive split on certain strain components. Additive decompositions are therefore not restricted to small deformations. Further, some of the existing formulations found in the literature are recovered as special cases of the proposed multiplicative split.

The remainder of this paper is organized as follows. Sec. 2 gives a brief overview of the general, curvilinear description of curved surfaces. Secs. 3 and 4 then discuss the kinematics and motion

of curved surfaces accounting for a multiplicative decomposition of the surface deformation gradient. This is followed by the presentation of the balance laws of mass, momentum, energy and entropy in Sec. 5. These lead to the coupled strong form problem statement, summarized in Sec. 6, and the general constitutive equations, derived in Sec. 7. The latter are illustrated by several examples for elastic and inelastic material behavior. Sec. 8 concludes the paper.

2 Mathematical surface description

This section gives a brief summary of the three-dimensional mathematical description of curved surfaces in the general framework of curvilinear coordinates. It allows to track any surface deformation (discussed in Sec. 3), and it is particularly suited for subsequent finite element formulations. In this framework, every point \mathbf{x} on a surface \mathcal{S} is given by the mapping

$$\mathbf{x} = \mathbf{x}(\xi^\alpha, t). \quad (1)$$

Here ξ^α , for $\alpha = 1, 2$, denotes the two curvilinear coordinates that can be associated with a 2D parameter domain \mathcal{P} as illustrated in Fig. 1, while $t \in [0, t_{\text{end}}]$ stands for time. Given (1), all

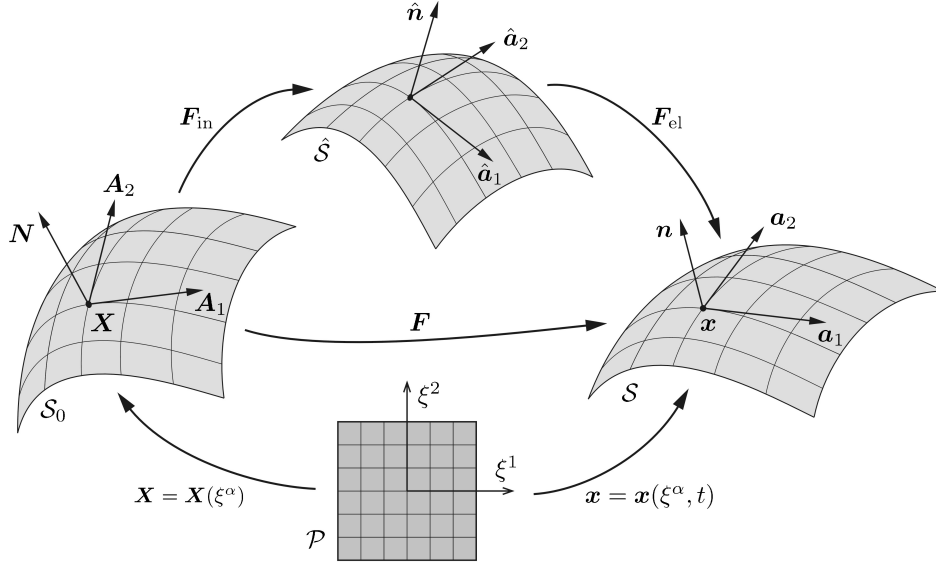


Figure 1: Surface description and kinematics: Multiplicative split into elastic and inelastic deformations and their relation to reference, intermediate and current configurations \mathcal{S}_0 , $\hat{\mathcal{S}}$ and \mathcal{S} .

geometrical aspects of the surface can be obtained. The tangent plane at $\mathbf{x} \in \mathcal{S}$ is characterized by the two tangent vectors

$$\mathbf{a}_\alpha := \frac{\partial \mathbf{x}}{\partial \xi^\alpha}, \quad (2)$$

while the surface normal at $\mathbf{x} \in \mathcal{S}$ is given by

$$\mathbf{n} = \frac{\mathbf{a}_1 \times \mathbf{a}_2}{\|\mathbf{a}_1 \times \mathbf{a}_2\|}. \quad (3)$$

The basis \mathbf{a}_1 , \mathbf{a}_2 and \mathbf{n} allows to introduce the notion of in-plane and out-of-plane surface objects. The tangent vectors \mathbf{a}_1 and \mathbf{a}_2 are generally not orthonormal, meaning that the so-called surface metric,

$$a_{\alpha\beta} := \mathbf{a}_\alpha \cdot \mathbf{a}_\beta, \quad (4)$$

generally gives $[a_{\alpha\beta}] \neq [1 \ 0; 0 \ 1]$. To restore orthonormality a set of dual tangent vectors \mathbf{a}^α is introduced from $\mathbf{a}_\alpha = a_{\alpha\beta} \mathbf{a}^\beta$ and $\mathbf{a}^\alpha = a^{\alpha\beta} \mathbf{a}_\beta$,³ where $[a^{\alpha\beta}] := [a_{\alpha\beta}]^{-1}$, such that $\mathbf{a}^\alpha \cdot \mathbf{a}_\beta = \delta_\beta^\alpha$ for $[\delta_\beta^\alpha] = [1 \ 0; 0 \ 1]$. This illustrates a very important property of $a_{\alpha\beta}$ and $a^{\alpha\beta}$: They lower or raise indices.

Another important surface characteristic is the curvature. It follows from the out-of-plane components of the second derivative $\mathbf{a}_{\alpha,\beta} := \partial \mathbf{a}_\alpha / \partial \xi^\beta$, denoted as

$$b_{\alpha\beta} := \mathbf{a}_{\alpha,\beta} \cdot \mathbf{n}. \quad (5)$$

These components can be arranged in the matrix $[b_\beta^\alpha] := [a^{\alpha\gamma} b_{\gamma\beta}]$, whose eigenvalues are the two principal surface curvatures

$$\kappa_\alpha = H \pm \sqrt{H^2 - \kappa}, \quad (6)$$

where

$$\begin{aligned} H &:= \frac{1}{2} a^{\alpha\beta} b_{\alpha\beta} \\ \kappa &:= \det[b_\beta^\alpha] \end{aligned} \quad (7)$$

are the mean curvature and Gaussian curvature of surface \mathcal{S} , respectively. The derivative $\mathbf{a}_{\alpha,\beta}$ is also referred to as the parametric derivate of \mathbf{a}_α . It is generally different to the so-called *co-variant derivative* of \mathbf{a}_α that is denoted by “ \cdot ” and defined as

$$\mathbf{a}_{\alpha;\beta} := (\mathbf{n} \otimes \mathbf{n}) \mathbf{a}_{\alpha,\beta}. \quad (8)$$

For general scalars and vectors (that have no free index) the parametric and co-variant derivatives are identical. Only for objects with free indices (such as \mathbf{a}_α and \mathbf{a}^α) a difference appears.

Analogous to (1), physical fields on \mathcal{S} are generally functions of ξ^α and t . Examples are surface density $\rho = \rho(\xi^\alpha, t)$ and surface temperature $T = T(\xi^\alpha, t)$. Their surface gradient follows from $\rho_{,\alpha} (= \rho_{;\alpha})$ and $T_{,\alpha} (= T_{;\alpha})$ as $\text{grad}_s \rho = \rho_{,\alpha} \mathbf{a}^\alpha$ and $\text{grad}_s T = T_{,\alpha} \mathbf{a}^\alpha$.

A more comprehensive treatment of the mathematical description of curved surfaces can be found in the classical textbooks on differential geometry, e.g. see [Kreyszig \(1991\)](#). A recent concise treatment is also provided in [Sauer \(2018\)](#).

3 Surface kinematics

This section introduces reference, current and intermediate configuration, and discusses the kinematical quantities between them. The discussion is restricted to Kirchhoff-Love kinematics. These are entirely based on the notion of surface strain and curvature, and do not need any further kinematical measures. The description follows the classical treatment found in the works by [Naghdi \(1972, 1982\)](#), [Pietraszkiewicz \(1989\)](#) and [Libai and Simmonds \(1998\)](#).

3.1 Classical kinematical measures

Suppose that the surface \mathcal{S} deforms over time. The initial configuration at time $t = 0$ is defined as reference configuration, and denoted \mathcal{S}_0 to distinguish it from the current configuration \mathcal{S} at time $t > 0$. In order to distinguish all the surface quantities introduced in Sec. 2, upper case symbols (or the subscript “0”) are used for the reference configuration, while lower case symbols

³Following index notation, summation (from 1 to 2) is implied on all terms with repeated Greek indices, i.e. $a^{\alpha\beta} \mathbf{a}_\beta = a^{\alpha 1} \mathbf{a}_1 + a^{\alpha 2} \mathbf{a}_2$.

(or no subscript) are used for the current configuration, see Fig. 1. The primary measure relating \mathcal{S} and \mathcal{S}_0 is the surface deformation gradient

$$\mathbf{F} := \mathbf{a}_\alpha \otimes \mathbf{A}^\alpha. \quad (9)$$

Together with its generalized inverse

$$\mathbf{F}^{-1} = \mathbf{A}_\alpha \otimes \mathbf{a}^\alpha, \quad (10)$$

it transforms the tangent vectors as

$$\begin{aligned} \mathbf{a}_\alpha &= \mathbf{F} \mathbf{A}_\alpha, \\ \mathbf{A}_\alpha &= \mathbf{F}^{-1} \mathbf{a}_\alpha, \\ \mathbf{A}^\alpha &= \mathbf{F}^\top \mathbf{a}^\alpha, \\ \mathbf{a}^\alpha &= \mathbf{F}^{-\top} \mathbf{A}^\alpha. \end{aligned} \quad (11)$$

From \mathbf{F} follow the two surface Cauchy Green tensors

$$\begin{aligned} \mathbf{C} &:= \mathbf{F}^\top \mathbf{F} = a_{\alpha\beta} \mathbf{A}^\alpha \otimes \mathbf{A}^\beta, \\ \mathbf{B} &:= \mathbf{F} \mathbf{F}^\top = A^{\alpha\beta} \mathbf{a}_\alpha \otimes \mathbf{a}_\beta. \end{aligned} \quad (12)$$

From these, the surface Green-Lagrange strain tensor

$$\mathbf{E} := \frac{1}{2}(\mathbf{C} - \mathbf{I}) \quad (13)$$

and the surface Almansi strain tensor

$$\mathbf{e} := \frac{1}{2}(\mathbf{i} - \mathbf{B}^{-1}), \quad (14)$$

can be defined. Here,

$$\begin{aligned} \mathbf{I} &:= \mathbf{A}_\alpha \otimes \mathbf{A}^\alpha = A_{\alpha\beta} \mathbf{A}^\alpha \otimes \mathbf{A}^\beta, \\ \mathbf{i} &:= \mathbf{a}_\alpha \otimes \mathbf{a}^\alpha = a_{\alpha\beta} \mathbf{a}^\alpha \otimes \mathbf{a}^\beta \end{aligned} \quad (15)$$

denote the surface identity tensors on \mathcal{S}_0 and \mathcal{S} , respectively. \mathbf{E} has the components

$$E_{\alpha\beta} := \mathbf{A}_\alpha \cdot \mathbf{E} \mathbf{A}_\beta = \frac{1}{2}(a_{\alpha\beta} - A_{\alpha\beta}), \quad (16)$$

w.r.t. basis \mathbf{A}^α , while \mathbf{e} has the components

$$e_{\alpha\beta} := \mathbf{a}_\alpha \cdot \mathbf{e} \mathbf{a}_\beta = \frac{1}{2}(a_{\alpha\beta} - A_{\alpha\beta}) \quad (17)$$

w.r.t. basis \mathbf{a}^α . To emphasize the equality $e_{\alpha\beta} = E_{\alpha\beta}$ and, as is seen later, the fact that the multiplicative split on \mathbf{F} leads to an additive split on these strain components, we introduce

$$\varepsilon_{\alpha\beta} := \frac{1}{2}(a_{\alpha\beta} - A_{\alpha\beta}), \quad (18)$$

such that

$$\begin{aligned} \mathbf{E} &= \varepsilon_{\alpha\beta} \mathbf{A}^\alpha \otimes \mathbf{A}^\beta, \\ \mathbf{e} &= \varepsilon_{\alpha\beta} \mathbf{a}^\alpha \otimes \mathbf{a}^\beta. \end{aligned} \quad (19)$$

Similar to (18), we introduce the relative curvature components

$$\kappa_{\alpha\beta} := b_{\alpha\beta} - B_{\alpha\beta}. \quad (20)$$

The surface Cauchy-Green tensors have two invariants, I_1 and J . In order to define them, the surface determinant of \mathbf{F} is introduced by

$$\det_s \mathbf{F} := \frac{\|\mathbf{F} \mathbf{V}_1 \times \mathbf{F} \mathbf{V}_2\|}{\|\mathbf{V}_1 \times \mathbf{V}_2\|} \quad (21)$$

for all non-parallel surface tangent vectors \mathbf{V}_1 and \mathbf{V}_2 (Javili et al., 2014). Picking $\mathbf{V}_\alpha = \mathbf{A}_\alpha$, this leads to the second invariant

$$J := \det_s \mathbf{F} = \frac{\|\mathbf{a}_1 \times \mathbf{a}_2\|}{\|\mathbf{A}_1 \times \mathbf{A}_2\|}, \quad (22)$$

which is equal to

$$J = \frac{\sqrt{\det[a_{\alpha\beta}]}}{\sqrt{\det[A_{\alpha\beta}]}} \quad (23)$$

and corresponds to the local change of area between \mathcal{S}_0 and \mathcal{S} . The first invariant is

$$I_1 = \mathbf{I} : \mathbf{C} = \mathbf{i} : \mathbf{B} = A^{\alpha\beta} a_{\alpha\beta}. \quad (24)$$

3.2 Kinematics of the multiplicative deformation split

The previous setting accounts only for a single deformation source. Its primary unknown is position \mathbf{x} , from which everything else follows. In order to extend the setting to deformations composed of two separate (i.e. elastic and inelastic) components, we introduce the intermediate surface configuration $\hat{\mathcal{S}}$ with the tangent vectors $\hat{\mathbf{a}}_\alpha$ that are now an additional set of unknowns. The deformation $\mathcal{S}_0 \rightarrow \hat{\mathcal{S}}$ is taken as the inelastic part, while $\hat{\mathcal{S}} \rightarrow \mathcal{S}$ is the elastic part, see Fig. 1. Given the tangent vectors $\hat{\mathbf{a}}_\alpha$, the surface normal $\hat{\mathbf{n}}$, metric $\hat{a}_{\alpha\beta}$, inverse metric $\hat{a}^{\alpha\beta}$, dual tangent vectors $\hat{\mathbf{a}}^\alpha$, curvature components $\hat{b}_{\alpha\beta}$, mean curvature \hat{H} and Gaussian curvature $\hat{\kappa}$ are obtained analogous to expressions (3)-(7) in Sec. 2. The introduced intermediate configuration $\hat{\mathcal{S}}$ implies that the surface deformation gradient \mathbf{F} can be multiplicatively split as

$$\mathbf{F} = \mathbf{F}_{\text{el}} \mathbf{F}_{\text{in}}, \quad (25)$$

where

$$\begin{aligned} \mathbf{F}_{\text{el}} &:= \mathbf{a}_\alpha \otimes \hat{\mathbf{a}}^\alpha, \\ \mathbf{F}_{\text{in}} &:= \hat{\mathbf{a}}_\alpha \otimes \mathbf{A}^\alpha \end{aligned} \quad (26)$$

are the elastic and inelastic surface deformation gradients, respectively. Split (25) implies the inverse split

$$\mathbf{F}^{-1} = \mathbf{F}_{\text{in}}^{-1} \mathbf{F}_{\text{el}}^{-1}, \quad (27)$$

with

$$\begin{aligned} \mathbf{F}_{\text{el}}^{-1} &:= \hat{\mathbf{a}}_\alpha \otimes \mathbf{a}^\alpha, \\ \mathbf{F}_{\text{in}}^{-1} &:= \mathbf{A}_\alpha \otimes \hat{\mathbf{a}}^\alpha. \end{aligned} \quad (28)$$

\mathbf{F}_{el} and \mathbf{F}_{in} transform the tangent vectors as

$$\begin{aligned} \mathbf{a}_\alpha &= \mathbf{F}_{\text{el}} \hat{\mathbf{a}}_\alpha, \\ \hat{\mathbf{a}}_\alpha &= \mathbf{F}_{\text{el}}^{-1} \mathbf{a}_\alpha, \\ \hat{\mathbf{a}}^\alpha &= \mathbf{F}_{\text{el}}^T \mathbf{a}^\alpha, \\ \mathbf{a}^\alpha &= \mathbf{F}_{\text{el}}^{-T} \hat{\mathbf{a}}^\alpha \end{aligned} \quad (29)$$

and

$$\begin{aligned}\hat{\mathbf{a}}_\alpha &= \mathbf{F}_{\text{in}} \mathbf{A}_\alpha, \\ \mathbf{A}_\alpha &= \mathbf{F}_{\text{in}}^{-1} \hat{\mathbf{a}}_\alpha, \\ \mathbf{A}^\alpha &= \mathbf{F}_{\text{in}}^T \hat{\mathbf{a}}^\alpha, \\ \hat{\mathbf{a}}^\alpha &= \mathbf{F}_{\text{in}}^{-T} \mathbf{A}^\alpha.\end{aligned}\tag{30}$$

These relations can be used to push forward the right surface Cauchy-Green tensor \mathbf{C} to the intermediate configuration, i.e.

$$\mathbf{C}_{\text{el}} := \mathbf{F}_{\text{in}}^{-T} \mathbf{C} \mathbf{F}_{\text{in}}^{-1} = \mathbf{F}_{\text{el}}^T \mathbf{F}_{\text{el}} = a_{\alpha\beta} \hat{\mathbf{a}}^\alpha \otimes \hat{\mathbf{a}}^\beta,\tag{31}$$

and to pull back the inverse left Cauchy-Green tensor \mathbf{B}^{-1} to the intermediate configuration, i.e.

$$\mathbf{B}_{\text{in}}^{-1} := \mathbf{F}_{\text{el}}^T \mathbf{B}^{-1} \mathbf{F}_{\text{el}} = \mathbf{F}_{\text{in}}^{-T} \mathbf{F}_{\text{in}}^{-1} = A_{\alpha\beta} \hat{\mathbf{a}}^\alpha \otimes \hat{\mathbf{a}}^\beta.\tag{32}$$

In order to decompose the strain, it is convenient to introduce the strain tensor

$$\hat{\mathbf{e}} := \varepsilon_{\alpha\beta} \hat{\mathbf{a}}^\alpha \otimes \hat{\mathbf{a}}^\beta\tag{33}$$

analogous to (19). This strain corresponds to the push forward of \mathbf{E} and the pull-back of \mathbf{e} to the intermediate configuration, since

$$\hat{\mathbf{e}} = \mathbf{F}_{\text{in}}^{-T} \mathbf{E} \mathbf{F}_{\text{in}}^{-1} = \mathbf{F}_{\text{el}}^T \mathbf{e} \mathbf{F}_{\text{el}}.\tag{34}$$

Inserting (13) or (14) into (34) gives

$$\hat{\mathbf{e}} = \frac{1}{2}(\mathbf{C}_{\text{el}} - \mathbf{B}_{\text{in}}^{-1})\tag{35}$$

which admits the simple additive decomposition

$$\hat{\mathbf{e}} = \hat{\mathbf{e}}_{\text{el}} + \hat{\mathbf{e}}_{\text{in}}\tag{36}$$

based on the definitions

$$\begin{aligned}\hat{\mathbf{e}}_{\text{el}} &:= \frac{1}{2}(\mathbf{C}_{\text{el}} - \hat{\mathbf{i}}) \\ \hat{\mathbf{e}}_{\text{in}} &:= \frac{1}{2}(\hat{\mathbf{i}} - \mathbf{B}_{\text{in}}^{-1})\end{aligned}\tag{37}$$

that are analogous to (13) and (14). Here,

$$\hat{\mathbf{i}} := \hat{\mathbf{a}}_\alpha \otimes \hat{\mathbf{a}}^\alpha = \hat{a}_{\alpha\beta} \hat{\mathbf{a}}^\alpha \otimes \hat{\mathbf{a}}^\beta\tag{38}$$

denotes the surface identity on $\hat{\mathcal{S}}$ analogous to (15). Introducing

$$\begin{aligned}\hat{\mathbf{e}}_{\text{el}} &= \varepsilon_{\alpha\beta}^{\text{el}} \hat{\mathbf{a}}^\alpha \otimes \hat{\mathbf{a}}^\beta, \\ \hat{\mathbf{e}}_{\text{in}} &= \varepsilon_{\alpha\beta}^{\text{in}} \hat{\mathbf{a}}^\alpha \otimes \hat{\mathbf{a}}^\beta\end{aligned}\tag{39}$$

then leads to the componentwise decomposition

$$\varepsilon_{\alpha\beta} = \varepsilon_{\alpha\beta}^{\text{el}} + \varepsilon_{\alpha\beta}^{\text{in}},\tag{40}$$

with

$$\begin{aligned}\varepsilon_{\alpha\beta}^{\text{el}} &= \frac{1}{2}(a_{\alpha\beta} - \hat{a}_{\alpha\beta}), \\ \varepsilon_{\alpha\beta}^{\text{in}} &= \frac{1}{2}(\hat{a}_{\alpha\beta} - A_{\alpha\beta}),\end{aligned}\tag{41}$$

which is analogous to (18). Thus we have showed that the multiplicative decomposition of \mathbf{F} generally leads to the additive decomposition of the intermediate strain tensor $\hat{\mathbf{e}}$. An alternative, but less insightful approach is to directly propose an additive decomposition of the strain

components without introducing $\mathbf{F} = \mathbf{F}_{\text{el}} \mathbf{F}_{\text{in}}$, as has for example been done by Reddy and Chin (1998) for thermoelastic shells, by Simo and Kennedy (1992) for elastoplastic shells, by Lubarda (2011) for viscoelastic shells, by Liang and Mahadevan (2011) for shell growth, by van der Sman (2015) for shell swelling, and by Roychowdhury and Gupta (2018) for surface defects. In the more general context of 3D continua, the additive decomposition (40)-(41) goes back to Sedov (1966)

We note that the proposed multiplicative split, apart from being more general than an additive split, equally applies to growth, swelling, viscosity, plasticity and thermal deformations, and thus allows for their unified treatment.

Likewise to decomposition (40), we introduce the additive curvature decomposition

$$\kappa_{\alpha\beta} = \kappa_{\alpha\beta}^{\text{el}} + \kappa_{\alpha\beta}^{\text{in}}, \quad (42)$$

with

$$\begin{aligned} \kappa_{\alpha\beta}^{\text{el}} &:= b_{\alpha\beta} - \hat{b}_{\alpha\beta}, \\ \kappa_{\alpha\beta}^{\text{in}} &:= \hat{b}_{\alpha\beta} - B_{\alpha\beta}. \end{aligned} \quad (43)$$

Due to split (25), the local area change, introduced in (22)-(23), becomes

$$J = J_{\text{el}} J_{\text{in}}, \quad (44)$$

with

$$\begin{aligned} J_{\text{el}} &= \det_s \mathbf{F}_{\text{el}} = \frac{\|\mathbf{a}_1 \times \mathbf{a}_2\|}{\|\hat{\mathbf{a}}_1 \times \hat{\mathbf{a}}_2\|} = \frac{\sqrt{\det[a_{\alpha\beta}]}}{\sqrt{\det[\hat{a}_{\alpha\beta}]}} , \\ J_{\text{in}} &= \det_s \mathbf{F}_{\text{in}} = \frac{\|\hat{\mathbf{a}}_1 \times \hat{\mathbf{a}}_2\|}{\|\mathbf{A}_1 \times \mathbf{A}_2\|} = \frac{\sqrt{\det[\hat{a}_{\alpha\beta}]}}{\sqrt{\det[A_{\alpha\beta}]} } . \end{aligned} \quad (45)$$

A further useful object is the first invariant of \mathbf{C}_{el} , given by the surface trace

$$I_1^{\text{el}} := \text{tr}_s \mathbf{C}_{\text{el}} = \mathbf{C}_{\text{el}} : \hat{\mathbf{i}} = \hat{a}^{\alpha\beta} a_{\alpha\beta}. \quad (46)$$

It is equivalent to the surface trace $\text{tr}_s \mathbf{B}_{\text{el}} = \mathbf{B}_{\text{el}} : \mathbf{i}$, where $\mathbf{B}_{\text{el}} = \mathbf{F}_{\text{el}} \mathbf{F}_{\text{el}}^{\text{T}}$.⁴ Likewise the first invariant of $\mathbf{C}_{\text{el}}^{-1}$ is given by

$$I_{1-}^{\text{el}} := \text{tr}_s \mathbf{C}_{\text{el}}^{-1} = \mathbf{C}_{\text{el}}^{-1} : \hat{\mathbf{i}} = a^{\alpha\beta} \hat{a}_{\alpha\beta} = \text{tr}_s \mathbf{B}_{\text{el}}^{-1} = \mathbf{B}_{\text{el}}^{-1} : \mathbf{i}. \quad (47)$$

Note, that in general $I_{1-}^{\text{el}} \neq 1/I_1^{\text{el}}$.

Remark 1: The inelastic deformation does not need to be compatible, i.e. \mathbf{F}_{in} does not need to follow as the gradient of a deformation mapping. Instead it can be treated as an independent unknown. For a recent discussion on incompatible plastic deformations, see Gupta et al. (2007).

Remark 2: A mutiplicative decomposition can also be used to split the elastic deformation into two parts, e.g. a pre-strain and an additional strain. In this case, the intermediate configuration $\hat{\mathcal{S}}$ is not stress-free but (pre-)stressed. The total stress then depends on the total strain in the usual way, and so the kinematical decomposition discussed above is not needed.

⁴Here, the surface trace of a surface tensor is defined w.r.t. the surface the tensor refers to.

3.3 Inelastic dilatation

For many applications, like growth or thermal expansion, the inelastic deformation is purely dilatational. Excluding rigid body rotations (which can be accounted for in the elastic deformation), inelastic dilatation is described by the intermediate tangent vectors

$$\hat{\mathbf{a}}_\alpha = \lambda_{\text{in}} \mathbf{A}_\alpha, \quad (48)$$

such that

$$\mathbf{F}_{\text{in}} = \lambda_{\text{in}} \mathbf{I}. \quad (49)$$

Here $\lambda_{\text{in}} = \sqrt{J_{\text{in}}}$ denotes the inelastic stretch. As a consequence,

$$\begin{aligned} \hat{a}_{\alpha\beta} &= J_{\text{in}} A_{\alpha\beta}, \\ \hat{a}^{\alpha\beta} &= A^{\alpha\beta} / J_{\text{in}} \end{aligned} \quad (50)$$

and $\hat{\mathbf{a}}^\alpha = \mathbf{A}^\alpha / \lambda_{\text{in}}$. From this follows

$$I_1^{\text{el}} = I_1 / J_{\text{in}}. \quad (51)$$

3.4 Inelastic isotropic bending

Analogous to inelastic dilatation is the case of inelastic isotropic bending. In this case, the two principal curvatures defined in (6) increase by the same scalar factor $\bar{\kappa}_{\text{in}}$ during inelastic deformation, i.e. the intermediate configuration is characterized by the principal curvatures

$$\hat{\kappa}_\alpha = \bar{\kappa}_{\text{in}} \kappa_{0\alpha}, \quad (52)$$

where $\kappa_{0\alpha}$ are the two principal curvatures of \mathcal{S}_0 . This implies

$$\hat{H} = \bar{\kappa}_{\text{in}} H_0, \quad \hat{\kappa} = \bar{\kappa}_{\text{in}}^2 \kappa_0. \quad (53)$$

This follows for example from considering the curvature relation

$$\hat{b}^\alpha_\beta = \bar{\kappa}_{\text{in}} B^\alpha_\beta, \quad (54)$$

which, together with (50), implies

$$\begin{aligned} \hat{b}_{\alpha\beta} &= J_{\text{in}} \bar{\kappa}_{\text{in}} B_{\alpha\beta}, \\ \hat{b}^{\alpha\beta} &= \bar{\kappa}_{\text{in}} B^{\alpha\beta} / J_{\text{in}}. \end{aligned} \quad (55)$$

4 Surface motion

The kinematical quantities introduced in the preceding section generally change over time, which is discussed in this section. To characterize these changes, we introduce the material time derivative

$$(\dot{\dots}) := \frac{d\dots}{dt} := \left. \frac{\partial \dots}{\partial t} \right|_{\mathbf{X} = \text{fixed}}. \quad (56)$$

From (1) thus follows the surface velocity $\mathbf{v} := \dot{\mathbf{x}}$. In the following two subsections, we summarize some of the consequences of (56) for the classical kinematical measures introduced in Sec. 3.1 and the kinematical decomposition of Sec. 3.2. While the expressions in Sec. 4.1 appear in older works, those of Sec. 4.2 are mostly new. They are required for formulating general constitutive models, as is discussed later (Sec. 7). Sec. 4.2 also exposes the coupling of elastic and inelastic contributions that are present in some of the kinematical quantities.

4.1 Classical measures of the surface motion

From definition (18) follows the strain rate

$$\dot{\varepsilon}_{\alpha\beta} = \frac{1}{2}\dot{a}_{\alpha\beta}, \quad (57)$$

where

$$\dot{a}_{\alpha\beta} = \dot{\mathbf{a}}_\alpha \cdot \mathbf{a}_\beta + \mathbf{a}_\alpha \cdot \dot{\mathbf{a}}_\beta, \quad (58)$$

according to (4). With this we can find the material time derivative of the area change J . Since $J = J(a_{\alpha\beta}) = J(\varepsilon_{\alpha\beta})$,⁵

$$\dot{J} = \frac{\partial J}{\partial a_{\alpha\beta}} \dot{a}_{\alpha\beta} = \frac{\partial J}{\partial \varepsilon_{\alpha\beta}} \dot{\varepsilon}_{\alpha\beta} \quad (59)$$

From (23) and (57) follows

$$\frac{\partial J}{\partial \varepsilon_{\alpha\beta}} = 2 \frac{\partial J}{\partial a_{\alpha\beta}} = J a^{\alpha\beta}, \quad (60)$$

so that

$$\frac{\dot{J}}{J} = \frac{1}{2} a^{\alpha\beta} \dot{a}_{\alpha\beta}. \quad (61)$$

Similarly, the first invariant of \mathbf{C} , $I_1 = I_1(a_{\alpha\beta}) = I_1(\varepsilon_{\alpha\beta})$, gives

$$\dot{I}_1 = \frac{\partial I_1}{\partial a_{\alpha\beta}} \dot{a}_{\alpha\beta} = \frac{\partial I_1}{\partial \varepsilon_{\alpha\beta}} \dot{\varepsilon}_{\alpha\beta}, \quad (62)$$

where

$$\frac{\partial I_1}{\partial \varepsilon_{\alpha\beta}} = 2 \frac{\partial I_1}{\partial a_{\alpha\beta}} = 2 A^{\alpha\beta}, \quad (63)$$

due to (24) and (57).

In order to express various curvature rates, we require

$$\dot{\mathbf{n}} = -(\mathbf{a}^\alpha \otimes \mathbf{n}) \dot{\mathbf{a}}_\alpha, \quad (64)$$

and

$$\dot{a}^{\alpha\beta} = \frac{\partial a^{\alpha\beta}}{\partial a_{\gamma\delta}} \dot{a}_{\gamma\delta}, \quad (65)$$

with

$$a^{\alpha\beta\gamma\delta} := \frac{\partial a^{\alpha\beta}}{\partial a_{\gamma\delta}} = -\frac{1}{2}(a^{\alpha\gamma} a^{\beta\delta} + a^{\alpha\delta} a^{\beta\gamma}), \quad (66)$$

see Sauer (2018). From (20) then follows the relative curvature rate

$$\dot{\kappa}_{\alpha\beta} = \dot{b}_{\alpha\beta}, \quad (67)$$

with

$$\dot{b}_{\alpha\beta} = \dot{\mathbf{a}}_{\alpha,\beta} \cdot \mathbf{n} + \mathbf{a}_{\alpha,\beta} \cdot \dot{\mathbf{n}}, \quad (68)$$

due to (5). Further, since $H = H(a_{\alpha\beta}, a_{\alpha\beta})$ and $\kappa = \kappa(a_{\alpha\beta}, a_{\alpha\beta})$, we find the mean curvature rate

$$\dot{H} = \frac{\partial H}{\partial a_{\alpha\beta}} \dot{a}_{\alpha\beta} + \frac{\partial H}{\partial b_{\alpha\beta}} \dot{b}_{\alpha\beta}, \quad (69)$$

with

$$\frac{\partial H}{\partial a_{\alpha\beta}} = -\frac{1}{2} b^{\alpha\beta}, \quad \frac{\partial H}{\partial b_{\alpha\beta}} = \frac{1}{2} a^{\alpha\beta}, \quad (70)$$

⁵To simplify notation, the same symbol (here J) is used for the variable and its different functions.

and the Gaussian curvature rate

$$\dot{\kappa} = \frac{\partial \kappa}{\partial a_{\alpha\beta}} \dot{a}_{\alpha\beta} + \frac{\partial \kappa}{\partial b_{\alpha\beta}} \dot{b}_{\alpha\beta}, \quad (71)$$

with

$$\frac{\partial \kappa}{\partial a_{\alpha\beta}} = -\kappa a^{\alpha\beta}, \quad \frac{\partial \kappa}{\partial b_{\alpha\beta}} = 2H a^{\alpha\beta} - b^{\alpha\beta}, \quad (72)$$

due to (7) and (65); see also Sauer (2018). Relations (57) and (67) obviously imply

$$\frac{\partial \dots}{\partial \varepsilon_{\alpha\beta}} = 2 \frac{\partial \dots}{\partial a_{\alpha\beta}}, \quad \frac{\partial \dots}{\partial \kappa_{\alpha\beta}} = \frac{\partial \dots}{\partial b_{\alpha\beta}}. \quad (73)$$

4.2 Decomposition of the surface motion

The additive strain decomposition of (40) and (41) directly leads to the additive rate decomposition

$$\begin{aligned} \dot{\varepsilon}_{\alpha\beta} &= \dot{\varepsilon}_{\alpha\beta}^{\text{el}} + \dot{\varepsilon}_{\alpha\beta}^{\text{in}}, \\ \dot{\varepsilon}_{\alpha\beta}^{\text{el}} &= \frac{1}{2} (\dot{a}_{\alpha\beta} - \dot{\hat{a}}_{\alpha\beta}), \\ \dot{\varepsilon}_{\alpha\beta}^{\text{in}} &= \frac{1}{2} \dot{\hat{a}}_{\alpha\beta}, \end{aligned} \quad (74)$$

where

$$\dot{\hat{a}}_{\alpha\beta} = \dot{\hat{a}}_{\alpha} \cdot \hat{a}_{\beta} + \hat{a}_{\alpha} \cdot \dot{\hat{a}}_{\beta}. \quad (75)$$

Also the multiplicative decomposition of J leads to an additive rate decomposition: From (44) directly follows

$$\frac{\dot{J}}{J} = \frac{\dot{J}_{\text{el}}}{J_{\text{el}}} + \frac{\dot{J}_{\text{in}}}{J_{\text{in}}}. \quad (76)$$

In order to determine \dot{J}_{el} and \dot{J}_{in} , we first note that for a general function $f(a_{\alpha\beta}, \hat{a}_{\alpha\beta}) = f(\varepsilon_{\alpha\beta}^{\text{el}}, \varepsilon_{\alpha\beta}^{\text{in}})$ we have⁶

$$\dot{f} = \frac{\partial f}{\partial a_{\alpha\beta}} \dot{a}_{\alpha\beta} + \frac{\partial f}{\partial \hat{a}_{\alpha\beta}} \dot{\hat{a}}_{\alpha\beta} = \frac{\partial f}{\partial \varepsilon_{\alpha\beta}^{\text{el}}} \dot{\varepsilon}_{\alpha\beta}^{\text{el}} + \frac{\partial f}{\partial \varepsilon_{\alpha\beta}^{\text{in}}} \dot{\varepsilon}_{\alpha\beta}^{\text{in}}. \quad (77)$$

From (74) then follows

$$\frac{\partial f}{\partial \varepsilon_{\alpha\beta}^{\text{el}}} = 2 \frac{\partial f}{\partial a_{\alpha\beta}}, \quad \frac{\partial f}{\partial \varepsilon_{\alpha\beta}^{\text{in}}} = 2 \frac{\partial f}{\partial a_{\alpha\beta}} + 2 \frac{\partial f}{\partial \hat{a}_{\alpha\beta}}. \quad (78)$$

Combing this with (73) leads to

$$\frac{\partial f}{\partial \varepsilon_{\alpha\beta}^{\text{el}}} = \frac{\partial f}{\partial \varepsilon_{\alpha\beta}}. \quad (79)$$

Applying (77) and (78) to $f = J_{\text{in}}(\hat{a}_{\alpha\beta}) = J_{\text{in}}(\varepsilon_{\alpha\beta}^{\text{in}})$ defined in (45.2) gives

$$\frac{\partial J_{\text{in}}}{\partial \varepsilon_{\alpha\beta}^{\text{el}}} = 0, \quad \frac{\partial J_{\text{in}}}{\partial \varepsilon_{\alpha\beta}^{\text{in}}} = J_{\text{in}} \hat{a}^{\alpha\beta} \quad (80)$$

and

$$\frac{\dot{J}_{\text{in}}}{J_{\text{in}}} = \frac{1}{2} \hat{a}^{\alpha\beta} \dot{\hat{a}}_{\alpha\beta}. \quad (81)$$

⁶Again the same symbol (here f) is used for the variable and its different functions.

Applying (77) and (78) to $f = J_{\text{el}}(a_{\alpha\beta}, \hat{a}_{\alpha\beta}) = J_{\text{el}}(\varepsilon_{\alpha\beta}^{\text{el}}, \varepsilon_{\alpha\beta}^{\text{in}})$ defined in (45.1) gives

$$\frac{\partial J_{\text{el}}}{\partial \varepsilon_{\alpha\beta}^{\text{el}}} = J_{\text{el}} a^{\alpha\beta}, \quad \frac{\partial J_{\text{el}}}{\partial \varepsilon_{\alpha\beta}^{\text{in}}} = J_{\text{el}} (a^{\alpha\beta} - \hat{a}^{\alpha\beta}) \quad (82)$$

and

$$\frac{\dot{J}_{\text{el}}}{J_{\text{el}}} = \frac{1}{2} a^{\alpha\beta} \dot{a}_{\alpha\beta} - \frac{1}{2} \hat{a}^{\alpha\beta} \dot{\hat{a}}_{\alpha\beta}. \quad (83)$$

The later equation agrees with (61), (76) and (81).

Applying (78) to $f = I_1^{\text{el}} = I_1^{\text{el}}(a_{\alpha\beta}, \hat{a}_{\alpha\beta}) = I_1^{\text{el}}(\varepsilon_{\alpha\beta}^{\text{el}}, \varepsilon_{\alpha\beta}^{\text{in}})$ defined in (46) gives

$$\frac{\partial I_1^{\text{el}}}{\partial \varepsilon_{\alpha\beta}^{\text{el}}} = 2 \hat{a}^{\alpha\beta}, \quad \frac{\partial I_1^{\text{el}}}{\partial \varepsilon_{\alpha\beta}^{\text{in}}} = 2 \hat{a}^{\alpha\beta\gamma\delta} (a_{\gamma\delta} - \hat{a}_{\gamma\delta}), \quad (84)$$

where

$$\hat{a}^{\alpha\beta\gamma\delta} := \frac{\partial \hat{a}^{\alpha\beta}}{\partial \hat{a}_{\gamma\delta}} = -\frac{1}{2} (\hat{a}^{\alpha\gamma} \hat{a}^{\beta\delta} + \hat{a}^{\alpha\delta} \hat{a}^{\beta\gamma}), \quad (85)$$

analogous to (66). I_1^{el} can then be obtained from (77).

Next we turn towards the curvature rates. The additive curvature decomposition in (42) and (43) leads to the additive rate decomposition

$$\begin{aligned} \dot{\kappa}_{\alpha\beta} &= \dot{\kappa}_{\alpha\beta}^{\text{el}} + \dot{\kappa}_{\alpha\beta}^{\text{in}}, \\ \dot{\kappa}_{\alpha\beta}^{\text{el}} &= \dot{b}_{\alpha\beta} - \dot{\hat{b}}_{\alpha\beta}, \\ \dot{\kappa}_{\alpha\beta}^{\text{in}} &= \dot{\hat{b}}_{\alpha\beta}, \end{aligned} \quad (86)$$

where

$$\dot{\hat{b}}_{\alpha\beta} = \dot{\hat{a}}_{\alpha,\beta} \cdot \hat{\mathbf{n}} + \hat{a}_{\alpha,\beta} \cdot \dot{\hat{\mathbf{n}}}, \quad (87)$$

and

$$\dot{\hat{\mathbf{n}}} = -(\hat{\mathbf{a}}^\alpha \otimes \hat{\mathbf{n}}) \dot{\hat{\mathbf{a}}}_\alpha, \quad (88)$$

analogous to (64) and (68). In order to find various curvature rates, we first note that for a general function $f(a_{\alpha\beta}, \hat{a}_{\alpha\beta}, b_{\alpha\beta}, \hat{b}_{\alpha\beta}) = f(\varepsilon_{\alpha\beta}^{\text{el}}, \varepsilon_{\alpha\beta}^{\text{in}}, \kappa_{\alpha\beta}^{\text{el}}, \kappa_{\alpha\beta}^{\text{in}})$ we have

$$\begin{aligned} \dot{f} &= \frac{\partial f}{\partial a_{\alpha\beta}} \dot{a}_{\alpha\beta} + \frac{\partial f}{\partial \hat{a}_{\alpha\beta}} \dot{\hat{a}}_{\alpha\beta} + \frac{\partial f}{\partial b_{\alpha\beta}} \dot{b}_{\alpha\beta} + \frac{\partial f}{\partial \hat{b}_{\alpha\beta}} \dot{\hat{b}}_{\alpha\beta}, \\ &= \frac{\partial f}{\partial \varepsilon_{\alpha\beta}^{\text{el}}} \dot{\varepsilon}_{\alpha\beta}^{\text{el}} + \frac{\partial f}{\partial \varepsilon_{\alpha\beta}^{\text{in}}} \dot{\varepsilon}_{\alpha\beta}^{\text{in}} + \frac{\partial f}{\partial \kappa_{\alpha\beta}^{\text{el}}} \dot{\kappa}_{\alpha\beta}^{\text{el}} + \frac{\partial f}{\partial \kappa_{\alpha\beta}^{\text{in}}} \dot{\kappa}_{\alpha\beta}^{\text{in}}. \end{aligned} \quad (89)$$

From (74) and (86) then follow

$$\frac{\partial f}{\partial \kappa_{\alpha\beta}^{\text{el}}} = \frac{\partial f}{\partial b_{\alpha\beta}}, \quad \frac{\partial f}{\partial \kappa_{\alpha\beta}^{\text{in}}} = \frac{\partial f}{\partial b_{\alpha\beta}} + \frac{\partial f}{\partial \hat{b}_{\alpha\beta}} \quad (90)$$

together with the already known expressions in (78). Combing this with (73) further leads to

$$\frac{\partial f}{\partial \kappa_{\alpha\beta}^{\text{el}}} = \frac{\partial f}{\partial \kappa_{\alpha\beta}^{\text{in}}}. \quad (91)$$

Applying (78) and (90) to $f = \hat{H}(\hat{a}_{\alpha\beta}, \hat{b}_{\alpha\beta}) = \hat{H}(\varepsilon_{\alpha\beta}^{\text{in}}, \kappa_{\alpha\beta}^{\text{in}})$ defined by $\hat{H} = \hat{a}^{\alpha\beta} \hat{b}_{\alpha\beta} / 2$ gives

$$\frac{\partial \hat{H}}{\partial \varepsilon_{\alpha\beta}^{\text{el}}} = 0, \quad \frac{\partial \hat{H}}{\partial \varepsilon_{\alpha\beta}^{\text{in}}} = -\hat{b}^{\alpha\beta}, \quad \frac{\partial \hat{H}}{\partial \kappa_{\alpha\beta}^{\text{el}}} = 0, \quad \frac{\partial \hat{H}}{\partial \kappa_{\alpha\beta}^{\text{in}}} = \frac{1}{2} \hat{a}^{\alpha\beta}, \quad (92)$$

analogous to (70). $\dot{\hat{H}}$ can then be obtained from (89).

Applying (78) and (90) to $f = \hat{\kappa}(\hat{a}_{\alpha\beta}, \hat{b}_{\alpha\beta}) = \hat{\kappa}(\varepsilon_{\alpha\beta}^{\text{in}}, \kappa_{\alpha\beta}^{\text{in}})$ defined by $\hat{\kappa} = \det[\hat{b}_{\alpha\beta}]/\det[\hat{a}_{\alpha\beta}]$ gives

$$\frac{\partial \hat{\kappa}}{\partial \varepsilon_{\alpha\beta}^{\text{el}}} = 0, \quad \frac{\partial \hat{\kappa}}{\partial \varepsilon_{\alpha\beta}^{\text{in}}} = -2\hat{\kappa} \hat{a}^{\alpha\beta}, \quad \frac{\partial \hat{\kappa}}{\partial \kappa_{\alpha\beta}^{\text{el}}} = 0, \quad \frac{\partial \hat{\kappa}}{\partial \kappa_{\alpha\beta}^{\text{in}}} = 2\hat{H} \hat{a}^{\alpha\beta} - \hat{b}^{\alpha\beta}, \quad (93)$$

analogous to (72). $\dot{\hat{\kappa}}$ can then be obtained from (89). The fact that the elastic derivatives in (92) and (93) are zero underlines the fact that the intermediate configuration is an independent unknown that is independent of $\varepsilon_{\alpha\beta}^{\text{el}}$ and $\kappa_{\alpha\beta}^{\text{el}}$.

On top of those expressions, the constitutive models discussed in Sec. 7 require the dependency of H and κ on the elastic and inelastic strain rates. Applying (78) and (90) to $f = H(a_{\alpha\beta}, b_{\alpha\beta}) = H(\varepsilon_{\alpha\beta}^{\text{el}}, \varepsilon_{\alpha\beta}^{\text{in}}, \kappa_{\alpha\beta}^{\text{el}}, \kappa_{\alpha\beta}^{\text{in}})$ defined by (7) gives

$$\frac{\partial H}{\partial \varepsilon_{\alpha\beta}^{\text{el}}} = \frac{\partial H}{\partial \varepsilon_{\alpha\beta}^{\text{in}}} = -b^{\alpha\beta}, \quad \frac{\partial H}{\partial \kappa_{\alpha\beta}^{\text{el}}} = \frac{\partial H}{\partial \kappa_{\alpha\beta}^{\text{in}}} = \frac{1}{2} a^{\alpha\beta}, \quad (94)$$

due to (70). Applying (78) and (90) to $f = \kappa(a_{\alpha\beta}, b_{\alpha\beta}) = \kappa(\varepsilon_{\alpha\beta}^{\text{el}}, \varepsilon_{\alpha\beta}^{\text{in}}, \kappa_{\alpha\beta}^{\text{el}}, \kappa_{\alpha\beta}^{\text{in}})$ defined by (7) gives

$$\frac{\partial \kappa}{\partial \varepsilon_{\alpha\beta}^{\text{el}}} = \frac{\partial \kappa}{\partial \varepsilon_{\alpha\beta}^{\text{in}}} = -2\kappa a^{\alpha\beta}, \quad \frac{\partial \kappa}{\partial \kappa_{\alpha\beta}^{\text{el}}} = \frac{\partial \kappa}{\partial \kappa_{\alpha\beta}^{\text{in}}} = 2H a^{\alpha\beta} - b^{\alpha\beta}, \quad (95)$$

due to (72).

5 Surface balance laws

This section discusses the balance laws of mass, momentum, energy and entropy for curved surfaces. The derivation follows the framework of Sauer and Duong (2017) and Sahu et al. (2017), which is based on the works by Prigogine (1961), de Groot and Mazur (1984), Naghdi (1972) and Steigmann (1999). It makes use of three important theorems: Reynold's transport theorem,

$$\frac{d}{dt} \int_{\mathcal{S}} \dots da = \int_{\mathcal{S}} \left((\dots) + \frac{\dot{J}}{J} (\dots) \right) da, \quad (96)$$

which follows from substituting $da = J dA$ and using the product rule, the surface divergence theorem,

$$\int_{\partial \mathcal{S}} \dots \nu_{\alpha} ds = \int_{\mathcal{S}} \dots ;_{\alpha} da, \quad (97)$$

where $\nu_{\alpha} = \mathbf{a}_{\alpha} \cdot \boldsymbol{\nu}$ is the in-plane component of the boundary normal $\boldsymbol{\nu}$ and $”;_{\alpha}$ is the co-variant derivative defined in Sec. 2, and the localization theorem

$$\int_{\mathcal{R}} \dots da = 0 \quad \forall \mathcal{R} \subset \mathcal{S} \quad \Leftrightarrow \quad \dots = 0 \quad \forall \mathbf{x} \in \mathcal{S}. \quad (98)$$

5.1 Surface mass balance

Mass balance is formulated here for the case of a mixture of two species. This could for example be a solvent diffusing into a matrix material and induce swelling. The partial surface densities $\rho_1 = \rho_1(\xi^{\alpha}, t)$ and $\rho_2 = \rho_2(\xi^{\alpha}, t)$ are introduced such that the current surface density of the mixture is $\rho = \rho_1 + \rho_2$ (with unit mass per current area).

5.1.1 Total mass balance

Consider the Lagrangian description of the total mass balance

$$\frac{d}{dt} \int_{\mathcal{R}} \rho \, da = \int_{\mathcal{R}} h \, da \quad \forall \mathcal{R} \subset \mathcal{S}, \quad (99)$$

where h is a surface mass source (mass per current area and time) that originates for example from growth or swelling. Applying Reynolds' transport theorem (96) and localization (98) gives

$$\dot{\rho} + \rho \dot{J}/J = h \quad \forall \mathbf{x} \in \mathcal{S}, \quad (100)$$

which is the governing ODE for ρ . In order to determine $\rho(t)$, the initial condition $\rho = \rho_0$ at $t = 0$ is required.

If $h = 0$, then $\rho = \rho_0/J$ solves ODE (100), which elegantly eliminates unknown ρ and its ODE. If $h \neq 0$, then ODE (100) needs to be solved (numerically). $h \neq 0$ induces growth, which is an inelastic deformation. An example is isotropic growth discussed in Sec. 7.3.1.

5.1.2 Partial mass balance

Additionally, the mass balance of the individual species needs to be accounted for. Given (100), it suffices to account for the mass balance of one species. We therefore introduce the relative concentration $\phi = \rho_1/\rho$ of species 1 and denote its source term h_1 . The partial mass balance thus is

$$\frac{d}{dt} \int_{\mathcal{R}} \rho \phi \, da = \int_{\mathcal{R}} h_1 \, da + \int_{\partial \mathcal{R}} j_\nu \, ds \quad \forall \mathcal{R} \subset \mathcal{S}, \quad (101)$$

where the j_ν term accounts for a relative mass flux of species 1 w.r.t. the average motion of the mixture. Defining the surface mass flux vector $\mathbf{j} = j^\alpha \mathbf{a}_\alpha$ through

$$j_\nu = -\mathbf{j} \cdot \boldsymbol{\nu} = -j^\alpha \nu_\alpha \quad (102)$$

and using the surface divergence theorem (97) on this term then leads to

$$\int_{\mathcal{R}} \left(\rho \dot{\phi} + \phi (\dot{\rho} + \rho \dot{J}/J) - h_1 + j^\alpha_{;\alpha} \right) da = 0 \quad \forall \mathcal{R} \subset \mathcal{S}. \quad (103)$$

Defining $h_1^* := h_1 - \phi h$ and making use of the localization theorem (98) and ODE (100), then gives

$$\rho \dot{\phi} = h_1^* - j^\alpha_{;\alpha} \quad \forall \mathbf{x} \in \mathcal{S}, \quad (104)$$

which is the governing ODE for the relative concentration ϕ . In order to determine $\phi(t)$, the initial condition $\phi = \phi_0$ at $t = 0$ is required. Interesting special cases for h_1^* are $h_1^* = h_1$ (the total mass is conserved), $h_1^* = (1 - \phi)h$ (only the mass of species 1 is increasing), $h_1^* = -\phi h$ (only the mass of species 2 is increasing) and $h_1^* = 0$ (the mass increase of species 1 and 2 has the ratio ϕ to $1 - \phi$).

5.2 Surface momentum balance

Before exploring momentum balance, the stress and bending moments of the shell have to be introduced. As shown in Sec. 5.2.1, these can be expressed w.r.t. the three configurations \mathcal{S} , \mathcal{S}_0 and $\hat{\mathcal{S}}$ – similar to the strains in Sec. 3.2. Based on this, linear and angular momentum balance are then discussed in Secs. 5.2.2 and 5.2.3.

5.2.1 Stress and moment tensors

For shells, the Cauchy stress tensor takes the form

$$\boldsymbol{\sigma} = N^{\alpha\beta} \mathbf{a}_\alpha \otimes \mathbf{a}_\beta + S^\alpha \mathbf{a}_\alpha \otimes \mathbf{n}, \quad (105)$$

with the in-plane membrane components $N^{\alpha\beta}$ and the out-of-plane shear components S^α . The traction vector on the boundary with normal $\boldsymbol{\nu} = \nu_\alpha \mathbf{a}^\alpha$ then follows from Cauchy's formula

$$\mathbf{T} = \boldsymbol{\sigma}^T \boldsymbol{\nu}. \quad (106)$$

Introducing

$$\mathbf{T}^\alpha := \boldsymbol{\sigma}^T \mathbf{a}^\alpha, \quad (107)$$

then leads to $\mathbf{T} = \mathbf{T}^\alpha \nu_\alpha$.

For later reference the surface tension,

$$\gamma := \frac{1}{2} \text{tr}_s \boldsymbol{\sigma} = \frac{1}{2} \boldsymbol{\sigma} : \mathbf{1} = \frac{1}{2} N^{\alpha\beta} a_{\alpha\beta}, \quad (108)$$

and the deviatoric surface stress,

$$\boldsymbol{\sigma}_{\text{dev}} := \boldsymbol{\sigma} - \gamma \mathbf{i}, \quad (109)$$

are introduced. The latter has the in-plane components

$$N_{\text{dev}}^{\alpha\beta} := N^{\alpha\beta} - \gamma a^{\alpha\beta} \quad (110)$$

in basis \mathbf{a}_α . The out-of-plane component S^α is identical for $\boldsymbol{\sigma}_{\text{dev}}$ and $\boldsymbol{\sigma}$.

The Cauchy stress describes the physical stress in configuration \mathcal{S} . It can be mapped to the (non-physical) second Piola-Kirchhoff stress tensor \mathbf{S} in configuration \mathcal{S}_0 using the classical pull-back formula

$$\mathbf{S} = J \tilde{\mathbf{F}}^{-1} \boldsymbol{\sigma} \tilde{\mathbf{F}}^{-T}, \quad (111)$$

where $\tilde{\mathbf{F}} := \mathbf{F} + \mathbf{n} \otimes \mathbf{N}$ is the full 3D deformation gradient for Kirchhoff-Love kinematics. In the same fashion we introduce the stress in configuration $\hat{\mathcal{S}}$ by

$$\hat{\boldsymbol{\sigma}} := J_{\text{el}} \tilde{\mathbf{F}}_{\text{el}}^{-1} \boldsymbol{\sigma} \tilde{\mathbf{F}}_{\text{el}}^{-T} \quad (112)$$

and note that

$$\mathbf{S} = J_{\text{in}} \tilde{\mathbf{F}}_{\text{in}}^{-1} \hat{\boldsymbol{\sigma}} \tilde{\mathbf{F}}_{\text{in}}^{-T}, \quad (113)$$

where $\tilde{\mathbf{F}}_{\text{el}} := \mathbf{F}_{\text{el}} + \mathbf{n} \otimes \hat{\mathbf{n}}$ and $\tilde{\mathbf{F}}_{\text{in}} := \mathbf{F}_{\text{in}} + \hat{\mathbf{n}} \otimes \mathbf{N}$. This lead to

$$\hat{\boldsymbol{\sigma}} = \hat{N}^{\alpha\beta} \hat{\mathbf{a}}_\alpha \otimes \hat{\mathbf{a}}_\beta + \hat{S}^\alpha \hat{\mathbf{a}}_\alpha \otimes \hat{\mathbf{n}} \quad (114)$$

and

$$\mathbf{S} = N_0^{\alpha\beta} \mathbf{A}_\alpha \otimes \mathbf{A}_\beta + S_0^\alpha \mathbf{A}_\alpha \otimes \mathbf{N}, \quad (115)$$

where $N_0^{\alpha\beta} := J_{\text{in}} \hat{N}^{\alpha\beta}$, $\hat{N}^{\alpha\beta} := J_{\text{el}} N^{\alpha\beta}$, $S_0^\alpha := J_{\text{in}} \hat{S}^\alpha$ and $\hat{S}^\alpha := J_{\text{el}} S^\alpha$.

Similar to the stress tensor $\boldsymbol{\sigma}$ and the traction vector \mathbf{T} , the bending moment tensor

$$\boldsymbol{\mu} = -M^{\alpha\beta} \mathbf{a}_\alpha \otimes \mathbf{a}_\beta \quad (116)$$

and the moment vector

$$\mathbf{M} = \boldsymbol{\mu}^T \boldsymbol{\nu} = M^\alpha \nu_\alpha, \quad (117)$$

with $M^\alpha = \boldsymbol{\mu}^T \mathbf{a}^\alpha$, are introduced in configuration \mathcal{S} . Just like $\boldsymbol{\sigma}$, $\boldsymbol{\mu}$ can be pulled back to $\hat{\mathcal{S}}$ and \mathcal{S}_0 by

$$\hat{\boldsymbol{\mu}} := J_{\text{el}} \tilde{\mathbf{F}}_{\text{el}}^{-1} \boldsymbol{\mu} \tilde{\mathbf{F}}_{\text{el}}^{-T} = -\hat{M}^{\alpha\beta} \hat{\mathbf{a}}_\alpha \otimes \hat{\mathbf{a}}_\beta \quad (118)$$

and

$$\boldsymbol{\mu}_0 := J \tilde{\mathbf{F}}^{-1} \boldsymbol{\mu} \tilde{\mathbf{F}}^{-T} = -M_0^{\alpha\beta} \mathbf{A}_\alpha \otimes \mathbf{A}_\beta, \quad (119)$$

where $M_0^{\alpha\beta} := J_{\text{in}} \hat{M}^{\alpha\beta}$ and $\hat{M}^{\alpha\beta} := J_{\text{el}} M^{\alpha\beta}$.

5.2.2 Linear surface momentum balance

The linear surface momentum balance is given by

$$\frac{d}{dt} \int_{\mathcal{R}} \rho \mathbf{v} da = \int_{\mathcal{R}} \mathbf{f} da + \int_{\partial \mathcal{R}} \mathbf{T} ds + \int_{\mathcal{R}} h \mathbf{v} da \quad \forall \mathcal{R} \subset \mathcal{S}, \quad (120)$$

where $\mathbf{v} := \dot{\mathbf{x}}$ is the current surface velocity, \mathbf{f} is a distributed surface load (force per current area) that, for two-species mixtures, has contributions acting on species 1 and 2 (i.e. $\mathbf{f} = \mathbf{f}_1 + \mathbf{f}_2$), \mathbf{T} is the traction vector on boundary $\partial \mathcal{R}$ and $h \mathbf{v}$ accounts for the momentum change of the added mass. Applying Reynolds' transport theorem (96), surface divergence theorem (97), localization (98) and ODE (100) gives

$$\mathbf{T}_{;\alpha}^\alpha + \mathbf{f} = \rho \dot{\mathbf{v}} \quad \forall \mathbf{x} \in \mathcal{S}, \quad (121)$$

which is the governing PDE for the motion. In order to determine $\mathbf{v}(t)$, the initial condition $\mathbf{v} = \mathbf{v}_0$ at $t = 0$ is required. In order to determine $\mathbf{x}(t)$, the additional initial condition $\mathbf{x} = \mathbf{X}$ at $t = 0$ is required. PDE (121) is exactly the same as for the mass conserving case, e.g. see Sauer and Duong (2017).

Remark 3: The surface load can also be defined per mass, i.e. $\mathbf{b} := \mathbf{f}/\rho$ and then decomposed as $\mathbf{f} = \rho \mathbf{b} = \rho_1 \mathbf{b}_1 + \rho_2 \mathbf{b}_2$ for the mixture. If $\mathbf{b}_1 = \mathbf{b}_2$, as for gravity, we find $\mathbf{b} = \mathbf{b}_1 = \mathbf{b}_2$.

5.2.3 Angular surface momentum balance

Also the angular surface momentum balance

$$\frac{d}{dt} \int_{\mathcal{R}} \mathbf{x} \times \rho \mathbf{v} da = \int_{\mathcal{R}} \mathbf{x} \times \mathbf{f} da + \int_{\partial \mathcal{R}} (\mathbf{x} \times \mathbf{T} + \mathbf{m}) ds + \int_{\mathcal{R}} \mathbf{x} \times h \mathbf{v} da \quad \forall \mathcal{R} \subset \mathcal{S}, \quad (122)$$

where $\mathbf{m} := \mathbf{n} \times \mathbf{M}$ is a distributed moment acting on boundary $\partial \mathcal{R}$, leads to the same local equations as before, i.e.

$$\begin{aligned} S^\alpha &= -M_{;\beta}^{\beta\alpha}, \\ \sigma^{\alpha\beta} &:= N^{\alpha\beta} - b_\gamma^\beta M^{\gamma\alpha} \text{ is symmetric} \end{aligned} \quad (123)$$

for all $\mathbf{x} \in \mathcal{S}$, e.g. see Sauer and Duong (2017).

5.3 Surface energy balance

The surface energy balance can be expressed as

$$\frac{d}{dt} \int_{\mathcal{R}} \rho e da = \int_{\mathcal{R}} \mathbf{v} \cdot \mathbf{f} da + \int_{\partial \mathcal{R}} (\mathbf{v} \cdot \mathbf{T} + \dot{\mathbf{n}} \cdot \mathbf{M}) ds + \int_{\mathcal{R}} h e da + \int_{\mathcal{R}} \rho r da + \int_{\partial \mathcal{R}} q_\nu ds \quad \forall \mathcal{R} \subset \mathcal{S}, \quad (124)$$

where

$$e = u + \frac{1}{2} \mathbf{v} \cdot \mathbf{v} \quad (125)$$

is the specific energy (per unit mass) at $\mathbf{x} \in \mathcal{B}$ that contains the stored energy u and the kinetic energy $\mathbf{v} \cdot \mathbf{v}/2$. The first two terms on the right hand side of (124) account for the mechanical power of the external forces \mathbf{f} and \mathbf{T} and external moment \mathbf{M} . The third term accounts for the power required to add mass h : power is needed to bring the added mass to energy level u

and velocity \mathbf{v} .⁷ The last two terms account for the thermal power of an external heat source r and a boundary influx q_ν . Defining the surface heat flux vector $\mathbf{q} = q^\alpha \mathbf{a}_\alpha$ through

$$q_\nu = -\mathbf{q} \cdot \boldsymbol{\nu} = -q^\alpha \nu_\alpha, \quad (126)$$

the surface divergence theorem gives

$$\int_{\partial\mathcal{R}} q_\nu \, ds = - \int_{\mathcal{R}} q_{;\alpha}^\alpha \, da. \quad (127)$$

Using the surface divergence theorem on the $\mathbf{v} \cdot \mathbf{T}$ term gives

$$\int_{\partial\mathcal{R}} \mathbf{v} \cdot \mathbf{T} \, ds = \int_{\mathcal{R}} (\mathbf{v} \cdot \mathbf{T}_{;\alpha}^\alpha + \frac{1}{2} \sigma^{\alpha\beta} \dot{a}_{\alpha\beta} + M^{\alpha\beta} \dot{b}_{\alpha\beta}) \, da - \int_{\partial\mathcal{R}} \dot{\mathbf{n}} \cdot \mathbf{M} \, ds, \quad (128)$$

see [Sahu et al. \(2017\)](#). Using these two equations, ODE (100) and PDE (121) then gives

$$\rho \dot{u} = \frac{1}{2} \sigma^{\alpha\beta} \dot{a}_{\alpha\beta} + M^{\alpha\beta} \dot{b}_{\alpha\beta} + \rho r - q_{;\alpha}^\alpha, \quad \forall \mathbf{x} \in \mathcal{S}, \quad (129)$$

which is the governing PDE for u . In order to determine $u(t)$, the initial condition $u = u_0$ at $t = 0$ is required. PDE (129) has the same format as in the classical case when $h = 0$ and no split of \mathbf{F} is considered ([Sahu et al., 2017](#)). But due to the split of \mathbf{F} , we can now write

$$\rho \dot{u} = \sigma^{\alpha\beta} (\dot{\varepsilon}_{\alpha\beta}^{\text{el}} + \dot{\varepsilon}_{\alpha\beta}^{\text{in}}) + M^{\alpha\beta} (\dot{\kappa}_{\alpha\beta}^{\text{el}} + \dot{\kappa}_{\alpha\beta}^{\text{in}}) + \rho r - q_{;\alpha}^\alpha, \quad \forall \mathbf{x} \in \mathcal{S}, \quad (130)$$

according to eqs. (57), (67), (74) and (86).

Remark 4: The $\frac{1}{2} \sigma^{\alpha\beta} \dot{a}_{\alpha\beta} \, da$ term can also be rewritten as

$$\frac{1}{2} \sigma^{\alpha\beta} \dot{a}_{\alpha\beta} \, da = \boldsymbol{\sigma} : \mathbf{D} \, da = \mathbf{S} : \dot{\mathbf{E}} \, dA, \quad (131)$$

where

$$\begin{aligned} \mathbf{D} &= \frac{1}{2} \dot{a}_{\alpha\beta} \mathbf{a}^\alpha \otimes \mathbf{a}^\beta, \\ \dot{\mathbf{E}} &= \frac{1}{2} \dot{a}_{\alpha\beta} \mathbf{A}^\alpha \otimes \mathbf{A}^\beta, \end{aligned} \quad (132)$$

are the symmetric velocity gradient (e.g. see [Sauer \(2018\)](#)) and the Green-Lagrange strain rate (following from (13)), respectively, and $\boldsymbol{\sigma}$ and \mathbf{S} are given by (105) and (111). This illustrates that the stress component $\sigma^{\alpha\beta}$ (and energy $\frac{1}{2} \sigma^{\alpha\beta} \dot{a}_{\alpha\beta}$) is expressed neither w.r.t. \mathcal{S}_0 nor \mathcal{S} , but directly w.r.t. parameter space \mathcal{P} ([Duong et al., 2017](#)). $\boldsymbol{\sigma}$ and \mathbf{S} , on the other hand are specific to \mathcal{S} and \mathcal{S}_0 , respectively.

Remark 5: In (124) the quantities e , \mathbf{f} , \mathbf{T} , \mathbf{M} , r and q_ν are defined for the common mixture in order to avoid dealing with partial quantities. In [Sahu et al. \(2017\)](#), on the other hand, \mathbf{f} is defined partially, such that the second term in (124) is the area integral over $\mathbf{v}_1 \cdot \rho_1 \mathbf{b}_1 + \mathbf{v}_2 \cdot \rho_2 \mathbf{b}_2$. This leads to an extra term in (129) and (130) if $\mathbf{b}_2 \neq \mathbf{b}_1$.

5.4 Surface entropy balance

The surface entropy balance is given by

$$\frac{d}{dt} \int_{\mathcal{R}} \rho s \, da = \int_{\mathcal{R}} (\rho \eta_e + \rho \eta_i + h s) \, da + \int_{\partial\mathcal{R}} \tilde{q}_\nu \, ds \quad \forall \mathcal{R} \subset \mathcal{S}, \quad (133)$$

⁷If the added mass carries initial, nonzero energy e_0 , this energy contribution can be accounted for in the ρr term. Alternatively, if one does not wish to account for e_0 in ρr , $h e$ in (124) should be replaced by $h(e - e_0)$.

where s is the specific entropy at $\mathbf{x} \in \mathcal{S}$, η_e is the external entropy production rate caused by external loads and heat sources, \tilde{q}_ν is an entropy influx on the boundary of the surface, $h s$ accounts for the entropy increase due to the added mass,⁸ and η_i is the internal entropy production rate, which according to the second law of thermodynamics satisfies

$$\eta_i \geq 0 \quad \forall \mathbf{x} \in \mathcal{S}. \quad (134)$$

Defining the surface entropy flux vector $\tilde{\mathbf{q}} = \tilde{q}^\alpha \mathbf{a}_\alpha$ through

$$\tilde{q}_\nu = -\tilde{\mathbf{q}} \cdot \boldsymbol{\nu} = -\tilde{q}^\alpha \nu_\alpha, \quad (135)$$

the surface divergence theorem and the localization theorem lead to the local equation

$$\rho \dot{s} = \rho \eta_e + \rho \eta_i - \tilde{q}_{;\alpha}^\alpha, \quad \forall \mathbf{x} \in \mathcal{S}, \quad (136)$$

which can be used to derive constitutive equations as is discussed in Sec. 7. For this, we introduce the Helmholtz free energy $\psi := u - Ts$, such that

$$\dot{s} = (\dot{u} - \dot{T}s - \dot{\psi})/T. \quad (137)$$

Here $T > 0$ is the absolute temperature. Inserting this and PDE (130) into (136) then gives

$$T\rho \dot{s} = \sigma^{\alpha\beta}(\dot{\varepsilon}_{\alpha\beta}^{\text{el}} + \dot{\varepsilon}_{\alpha\beta}^{\text{in}}) + M^{\alpha\beta}(\dot{\kappa}_{\alpha\beta}^{\text{el}} + \dot{\kappa}_{\alpha\beta}^{\text{in}}) + \rho r - T\left(\frac{q^\alpha}{T}\right)_{;\alpha} - \frac{q^\alpha T_{;\alpha}}{T} - \rho \dot{T}s - \rho \dot{\psi}. \quad (138)$$

In deriving this equation we have used local energy balance (129), which in turn uses local mass balance (100) and local momentum balance (121). We have thus used all PDEs apart from the local concentration balance (104). In order to account for it we add it to the right hand side of (138) using the Lagrange multiplier method, i.e.

$$T\rho \dot{s} = \dots + \mu(\rho \dot{\phi} - h_1^* + j_{;\alpha}^\alpha), \quad (139)$$

where μ is the Lagrange multiplier that corresponds to the chemical potential as will be shown later. The last term in (139) can be rewritten as

$$\mu j_{;\alpha}^\alpha = T\left(\frac{\mu j^\alpha}{T}\right)_{;\alpha} - T j^\alpha \left(\frac{\mu}{T}\right)_{;\alpha} \quad (140)$$

in order to combine it with the $T(q^\alpha/T)_{;\alpha}$ term. We thus find

$$\begin{aligned} T\rho \dot{s} = & \rho r - \mu h_1^* - T\left(\frac{q^\alpha}{T} - \frac{\mu j^\alpha}{T}\right)_{;\alpha} + \sigma^{\alpha\beta}(\dot{\varepsilon}_{\alpha\beta}^{\text{el}} + \dot{\varepsilon}_{\alpha\beta}^{\text{in}}) + M^{\alpha\beta}(\dot{\kappa}_{\alpha\beta}^{\text{el}} + \dot{\kappa}_{\alpha\beta}^{\text{in}}) \\ & - \rho s \dot{T} - \frac{q^\alpha T_{;\alpha}}{T} + \rho \mu \dot{\phi} - T j^\alpha \left(\frac{\mu}{T}\right)_{;\alpha} - \rho \dot{\psi}. \end{aligned} \quad (141)$$

On the right hand side here, the only source terms are the first two terms, while the only divergence-like term is the third term. Comparing this with (136), we can thus identify $\eta_e = r/T - \mu h_1^*/(T\rho)$ and $\tilde{q}^\alpha = q^\alpha/T - \mu j^\alpha/T$, such that the second law (134) yields

$$T\rho \eta_i = \sigma^{\alpha\beta}(\dot{\varepsilon}_{\alpha\beta}^{\text{el}} + \dot{\varepsilon}_{\alpha\beta}^{\text{in}}) + M^{\alpha\beta}(\dot{\kappa}_{\alpha\beta}^{\text{el}} + \dot{\kappa}_{\alpha\beta}^{\text{in}}) - \rho s \dot{T} - \frac{q^\alpha T_{;\alpha}}{T} + \rho \mu \dot{\phi} - T j^\alpha \left(\frac{\mu}{T}\right)_{;\alpha} - \rho \dot{\psi} \geq 0. \quad (142)$$

⁸If the added mass carries initial, nonzero entropy, this additional entropy contribution can be accounted for in the $\rho \eta_e$ term.

6 Problem statement

In this work we consider the case of coupling elastic deformations with either growth, swelling, viscosity, plasticity or thermal deformation. So there is only coupling of two deformation types. In principle three and more types can also be coupled. This would require introducing further intermediate configurations. This section discusses the strong form for the coupled two-field problem. The recovery of the intermediate configuration is also addressed.

6.1 Strong form

The strong form can be unified by the problem statement: Find $\mathbf{x}(\xi^\alpha, t)$, $\hat{\mathbf{a}}_{\alpha\beta}(\xi^\gamma, t)$ and $\hat{\mathbf{b}}_{\alpha\beta}(\xi^\gamma, t)$ satisfying PDE (121) and,

- for growth, ODE (100). In this case, $\hat{\mathbf{a}}_{\alpha\beta}$ and $\hat{\mathbf{b}}_{\alpha\beta}$ are either prescribed or defined through ρ . So the primary unknowns are \mathbf{x} and ρ . Examples are given by Eqs. (50), (55), (160) and (164).
- for swelling, PDE (104). In this case, $\hat{\mathbf{a}}_{\alpha\beta}$ and $\hat{\mathbf{b}}_{\alpha\beta}$ are defined through ϕ , e.g. by (50), (55), (165) and (166), and so the primary unknowns are \mathbf{x} and ϕ . If the swelling is not mass conserving (i.e. $h \neq 0$), ρ is also unknown and needs to be obtained from ODE (100).
- for viscoelasticity and elastoplasticity, an evolution law (ODE) for $\hat{\mathbf{a}}_{\alpha\beta}$ and $\hat{\mathbf{b}}_{\alpha\beta}$, like (185), (205), (214) or (223).
- for thermoelasticity, PDE (130). In this case, $\hat{\mathbf{a}}_{\alpha\beta}$ and $\hat{\mathbf{b}}_{\alpha\beta}$ are defined through T , e.g. by (50), (55), (227) and (228), and so the primary unknowns are \mathbf{x} and T .

In general, the governing ODEs and PDEs are nonlinear and coupled, and hence need to be solved numerically. The ODEs can be solved locally using numerical integration schemes like the implicit Euler scheme. The problem simplifies if ρ , ϕ or T are prescribed. In those cases the problem decouples. In order to fully characterize PDEs (104), (121) and (129), constitutive expressions for the mass flux, stress, bending moments and heat flux are needed. Those are discussed in Sec. 7.

6.2 Recovery of $\hat{\mathbf{a}}_\alpha$

Strictly the recovery of $\hat{\mathbf{a}}_1$ and $\hat{\mathbf{a}}_2$, which fully define the intermediate configuration $\hat{\mathcal{S}}$, is not needed to solve the problem, but it may still be interesting to reconstruct $\hat{\mathbf{a}}_\alpha$, and from it \mathbf{F}_{in} , for various reasons.

The recovery is straightforward for isotropic growth, isotropic swelling and isotropic thermal expansion, since in these cases $\hat{\mathbf{a}}_\alpha$ is given by (48), with λ_{in} being either prescribed directly or defined through ρ , ϕ or T , as in some of the examples of Sec. 7.3.

For viscoelasticity and elastoplasticity, on the other hand, the two vectors $\hat{\mathbf{a}}_1$ and $\hat{\mathbf{a}}_2$ can be determined from the two equations

$$\begin{aligned}\hat{\mathbf{a}}_{\alpha\beta} &= \hat{\mathbf{a}}_\alpha \cdot \hat{\mathbf{a}}_\beta \\ \hat{\mathbf{b}}_{\alpha\beta} &= \hat{\mathbf{a}}_{\alpha,\beta} \cdot \hat{\mathbf{n}}\end{aligned}\tag{143}$$

that each have three cases. In order to eliminate rigid body rotations, $\hat{\mathbf{a}}_1$ and $\hat{\mathbf{a}}_2$ need to be fixed at some point.

Remark 6: If no inelastic bending occurs, i.e. $\hat{\mathbf{n}} = \mathbf{N}$, the second equation can be replaced by the scalar equation

$$\hat{\mathbf{a}}_\alpha \cdot \mathbf{N} = 0, \quad (144)$$

that has two cases and fixes the inclination of $\hat{\mathcal{S}}$, and the condition

$$(\hat{\mathbf{a}}_1 \times \hat{\mathbf{a}}_2) \cdot \mathbf{N} = \|\hat{\mathbf{a}}_1 \times \hat{\mathbf{a}}_2\| \quad (145)$$

that fixes the orientation of $\hat{\mathcal{S}}$. Additionally, $\hat{\mathbf{a}}_1$ (or $\hat{\mathbf{a}}_2$) needs to be fixed at a point to eliminate the rigid body rotation around \mathbf{N} .

7 Constitution

This section derives the constitutive equations following from the second law of thermodynamics and provides various examples for growth, swelling, elasticity, viscosity, plasticity and thermal expansion.

7.1 Constitutive theory

In general, the Helmholtz free energy is supposed to be a function of the elastic strains $\varepsilon_{\alpha\beta}^{\text{el}}$ and $\kappa_{\alpha\beta}^{\text{el}}$, temperature T and concentration ϕ , i.e.

$$\psi = \psi(\varepsilon_{\alpha\beta}^{\text{el}}, \kappa_{\alpha\beta}^{\text{el}}, T, \phi), \quad (146)$$

such that

$$\dot{\psi} = \frac{\partial \psi}{\partial \varepsilon_{\alpha\beta}^{\text{el}}} \dot{\varepsilon}_{\alpha\beta}^{\text{el}} + \frac{\partial \psi}{\partial \kappa_{\alpha\beta}^{\text{el}}} \dot{\kappa}_{\alpha\beta}^{\text{el}} + \frac{\partial \psi}{\partial T} \dot{T} + \frac{\partial \psi}{\partial \phi} \dot{\phi}. \quad (147)$$

Eq. (142) then yields⁹

$$\begin{aligned} T\rho\eta_{\text{i}} &= \left(\sigma^{\alpha\beta} - \rho \frac{\partial \psi}{\partial \varepsilon_{\alpha\beta}^{\text{el}}} \right) \dot{\varepsilon}_{\alpha\beta}^{\text{el}} + \sigma^{\alpha\beta} \dot{\varepsilon}_{\alpha\beta}^{\text{in}} \\ &+ \left(M^{\alpha\beta} - \rho \frac{\partial \psi}{\partial \kappa_{\alpha\beta}^{\text{el}}} \right) \dot{\kappa}_{\alpha\beta}^{\text{el}} + M^{\alpha\beta} \dot{\kappa}_{\alpha\beta}^{\text{in}} \\ &- \rho \left(s + \frac{\partial \psi}{\partial T} \right) \dot{T} - T \frac{q^{\alpha} T_{;\alpha}}{T} \\ &+ \rho \left(\mu - \frac{\partial \psi}{\partial \phi} \right) \dot{\phi} - T j^{\alpha} \left(\frac{\mu}{T} \right)_{;\alpha} \geq 0. \end{aligned} \quad (148)$$

We now invoke the procedure of Coleman and Noll (1964). Two cases have to be considered. The first case supposes that $\varepsilon_{\alpha\beta}^{\text{in}}$ and $\kappa_{\alpha\beta}^{\text{in}}$ are independent process variables. Then, since (148) is true for all rates $\dot{\varepsilon}_{\alpha\beta}^{\text{el}}, \dot{\varepsilon}_{\alpha\beta}^{\text{in}}, \dot{\kappa}_{\alpha\beta}^{\text{el}}, \dot{\kappa}_{\alpha\beta}^{\text{in}}, \dot{T}, \dot{\phi}$ and gradients $T_{;\alpha}, (\mu/T)_{;\alpha}$, we obtain the sufficient

⁹Replacing $\dot{\varepsilon}_{\alpha\beta}^{\text{el}}$ according to (74.1), Eq. (148) can be also expressed in terms of $\dot{\varepsilon}_{\alpha\beta}$ and $\dot{\varepsilon}_{\alpha\beta}^{\text{in}}$.

conditions¹⁰

$$\begin{aligned}
\sigma^{\alpha\beta} &= \rho \frac{\partial \psi}{\partial \varepsilon_{\alpha\beta}^{\text{el}}}, & \sigma^{\alpha\beta} \dot{\varepsilon}_{\alpha\beta}^{\text{in}} &\geq 0, \\
M^{\alpha\beta} &= \rho \frac{\partial \psi}{\partial \kappa_{\alpha\beta}^{\text{el}}}, & M^{\alpha\beta} \dot{\kappa}_{\alpha\beta}^{\text{in}} &\geq 0, \\
s &= -\frac{\partial \psi}{\partial T}, & q^\alpha T_{;\alpha} &\leq 0, \\
\mu &= \frac{\partial \psi}{\partial \phi}, & j^\alpha \left(\frac{\mu}{T} \right)_{;\alpha} &\leq 0,
\end{aligned} \tag{149}$$

which are the general constitutive relations for the stresses $\sigma^{\alpha\beta}$, bending moments $M^{\alpha\beta}$, inelastic strains $\varepsilon_{\alpha\beta}^{\text{in}}$, inelastic curvature change $\kappa_{\alpha\beta}^{\text{in}}$, heat flux q^α , entropy s , concentration flux j^α and Lagrange multiplier μ . The latter is identified to be the chemical potential.

On the other hand, if $\dot{\varepsilon}_{\alpha\beta}^{\text{in}}$ and $\dot{\kappa}_{\alpha\beta}^{\text{in}}$ are functions of T and ϕ , their rates can be expanded into

$$\begin{aligned}
\dot{\varepsilon}_{\alpha\beta}^{\text{in}} &= \frac{\partial \varepsilon_{\alpha\beta}^{\text{in}}}{\partial T} \dot{T} + \frac{\partial \varepsilon_{\alpha\beta}^{\text{in}}}{\partial \phi} \dot{\phi}, \\
\dot{\kappa}_{\alpha\beta}^{\text{in}} &= \frac{\partial \kappa_{\alpha\beta}^{\text{in}}}{\partial T} \dot{T} + \frac{\partial \kappa_{\alpha\beta}^{\text{in}}}{\partial \phi} \dot{\phi}.
\end{aligned} \tag{150}$$

Inserting this into (148) then yields

$$\begin{aligned}
T \rho \eta_{\text{i}} &= \left(\sigma^{\alpha\beta} - \rho \frac{\partial \psi}{\partial \varepsilon_{\alpha\beta}^{\text{el}}} \right) \dot{\varepsilon}_{\alpha\beta}^{\text{el}} + \left(M^{\alpha\beta} - \rho \frac{\partial \psi}{\partial \kappa_{\alpha\beta}^{\text{el}}} \right) \dot{\kappa}_{\alpha\beta}^{\text{el}} \\
&\quad - \rho \left(s + \frac{\partial \psi}{\partial T} - \frac{\sigma^{\alpha\beta}}{\rho} \frac{\partial \varepsilon_{\alpha\beta}^{\text{in}}}{\partial T} - \frac{M^{\alpha\beta}}{\rho} \frac{\partial \kappa_{\alpha\beta}^{\text{in}}}{\partial T} \right) \dot{T} - T \frac{q^\alpha T_{;\alpha}}{T} \\
&\quad + \rho \left(\mu - \frac{\partial \psi}{\partial \phi} + \frac{\sigma^{\alpha\beta}}{\rho} \frac{\partial \varepsilon_{\alpha\beta}^{\text{in}}}{\partial \phi} + \frac{M^{\alpha\beta}}{\rho} \frac{\partial \kappa_{\alpha\beta}^{\text{in}}}{\partial \phi} \right) \dot{\phi} - T j^\alpha \left(\frac{\mu}{T} \right)_{;\alpha} \geq 0.
\end{aligned} \tag{151}$$

Since this is true for all $\dot{\varepsilon}_{\alpha\beta}^{\text{el}}$, $\dot{\kappa}_{\alpha\beta}^{\text{el}}$, \dot{T} , $\dot{\phi}$, $T_{;\alpha}$ and $(\mu/T)_{;\alpha}$, we now find

$$\begin{aligned}
s &= -\frac{\partial \psi}{\partial T} + \frac{\sigma^{\alpha\beta}}{\rho} \frac{\partial \varepsilon_{\alpha\beta}^{\text{in}}}{\partial T} + \frac{M^{\alpha\beta}}{\rho} \frac{\partial \kappa_{\alpha\beta}^{\text{in}}}{\partial T}, \\
\mu &= \frac{\partial \psi}{\partial \phi} - \frac{\sigma^{\alpha\beta}}{\rho} \frac{\partial \varepsilon_{\alpha\beta}^{\text{in}}}{\partial \phi} - \frac{M^{\alpha\beta}}{\rho} \frac{\partial \kappa_{\alpha\beta}^{\text{in}}}{\partial \phi},
\end{aligned} \tag{152}$$

together with the equations for $\sigma^{\alpha\beta}$ and $M^{\alpha\beta}$ and the inequality conditions for q^α and j^α already listed in (149). Now, the conditions $\sigma^{\alpha\beta} \dot{\varepsilon}_{\alpha\beta}^{\text{in}} \geq 0$ and $M^{\alpha\beta} \dot{\kappa}_{\alpha\beta}^{\text{in}} \geq 0$ are no longer a requirement. As (152) shows for the second case, the entropy and chemical potential have contributions coming from the inelastic deformation measures $\varepsilon_{\alpha\beta}^{\text{in}}$ and $\kappa_{\alpha\beta}^{\text{in}}$.

7.2 Alternative constitutive description

By redefining the Helmholtz free energy, we can rewrite some of the above constitutive equations. Since the Helmholtz free energy ψ is defined per unit mass, the total energy is

$$\Pi := \int_{\mathcal{M}} \psi \, \text{d}m = \int_S \rho \psi \, \text{d}a, \tag{153}$$

¹⁰They are not necessary conditions as they can be combined into new conditions.

where the first integral denotes the integration over the total mass of surface \mathcal{S} . Defining ρ^0 as the current density in the reference configuration, i.e. $\rho^0 := J \rho$, we can also write

$$\Pi = \int_{\mathcal{S}_0} \rho^0 \psi \, dA. \quad (154)$$

Due to growth ($h \neq 0$), density ρ^0 is changing over time and is not equal to the initial density ρ_0 (unless $h = 0$). Likewise, we introduce $\hat{\rho}$ as the density in $\hat{\mathcal{S}}$, i.e. $\hat{\rho} := J_{\text{el}} \rho$, so that we can further write

$$\Pi = \int_{\hat{\mathcal{S}}} \hat{\rho} \psi \, d\hat{a} = \int_{\hat{\mathcal{S}}} \hat{\Psi} \, d\hat{a}, \quad (155)$$

where $d\hat{a} = J_{\text{in}} dA$ and

$$\hat{\Psi} := \hat{\rho} \psi \quad (156)$$

is the Helmholtz free energy per unit intermediate area. Since $\hat{\rho}$ is independent of the elastic deformation (as long as $\hat{h} = J_{\text{el}} h$ is),¹¹ we can rewrite the constitutive laws for $\sigma^{\alpha\beta}$ and $M^{\alpha\beta}$ into

$$\begin{aligned} \sigma_{(\text{el})}^{\alpha\beta} &= \frac{1}{J_{\text{el}}} \frac{\partial \hat{\Psi}}{\partial \varepsilon_{\alpha\beta}^{\text{el}}}, \\ M_{(\text{el})}^{\alpha\beta} &= \frac{1}{J_{\text{el}}} \frac{\partial \hat{\Psi}}{\partial \kappa_{\alpha\beta}^{\text{el}}}. \end{aligned} \quad (157)$$

Subscript “(el)” is added here to indicate that this is the stress following from the elasticity model. But since $\sigma_{(\text{el})}^{\alpha\beta} = \sigma_{(\text{in})}^{\alpha\beta} = \sigma^{\alpha\beta}$, brackets on this subscript are used. Using the alternative stress measures introduced in (114) and using identities (79) and (91), we can further write

$$\begin{aligned} \hat{\sigma}_{(\text{el})}^{\alpha\beta} &= \frac{\partial \hat{\Psi}}{\partial \varepsilon_{\alpha\beta}^{\text{el}}} = \frac{\partial \hat{\Psi}}{\partial \varepsilon_{\alpha\beta}}, \\ \hat{M}_{(\text{el})}^{\alpha\beta} &= \frac{\partial \hat{\Psi}}{\partial \kappa_{\alpha\beta}^{\text{el}}} = \frac{\partial \hat{\Psi}}{\partial \kappa_{\alpha\beta}}. \end{aligned} \quad (158)$$

7.3 Constitutive examples

The following subsections give examples for the elastic and inelastic material behavior of curved surfaces resulting from the constitutive laws in (149), (152) and (157). We therefore consider that the Helmholtz free energy has additive mechanical, thermal and concentrational parts, i.e.

$$\psi = \psi_{\text{mech}} + \psi_{\text{therm}} + \psi_{\text{conc}}. \quad (159)$$

An additional energy due to growth is not required since the energy change due to mass changes is already accounted for in Π through ρ , see (153).

7.3.1 Growth models

i. Isotropic in-plane growth: In this case $\hat{\mathbf{a}}_\alpha$ and \mathbf{F}_{in} are given by (48) and (49). If this growth is unrestricted and maintains constant density over time, i.e. $J_{\text{el}} = 1$ and $\rho = \rho_0 = \text{const.} \, \forall t$, ODE (100) leads to the exponential growth law

$$J_{\text{in}} = J_0 \exp(h t / \rho_0), \quad (160)$$

¹¹We can rewrite ODE (100) into $\dot{\rho} + \hat{\rho} \dot{J}_{\text{in}} / J_{\text{in}} - \hat{h} = 0$.

where J_0 is a dimensionless constant. In case of restricted growth at changing density ($J_{\text{el}} \neq 1$, $\rho \neq \text{const.}$), expression (160) can still be used as a possible model. However in that case, also other growth models in the form

$$J_{\text{in}} = J_{\text{in}}(t) \quad (161)$$

are possible. Examples are linear¹² growth in h ,

$$J_{\text{in}} = J_0 (1 + c h t)^2, \quad (162)$$

and logarithmic expansion in time,

$$J_{\text{in}} = J_0 (1 + \ln(1 + t/t_0)), \quad (163)$$

where J_0 , c and t_0 are constants. No matter what growth model is used, if ρ is not assumed constant, it has to be solved for from ODE (100). If growth is mass conserving, e.g. during expansion (163), $\rho = \rho_0/J$ solves ODE (100). Given J_{in} , $\hat{a}_{\alpha\beta}$ is then fully defined via (50).

ii. Curvature growth: An example for curvature growth is the isotopic bending model (52) with the linear increase

$$\bar{\kappa}_{\text{in}} = 1 + c h t, \quad (164)$$

that could be caused by a one-sided mass source h . $\hat{b}_{\alpha\beta}$ is then given by (55).

7.3.2 Models for concentration induced swelling and diffusion

i. Linear isotropic swelling: A classical model for swelling is the linear model

$$J_{\text{in}} = \lambda_{\text{in}}^2, \quad \lambda_{\text{in}} = 1 + \alpha_c (\phi - \phi_0), \quad (165)$$

where the material constant α_c denotes the coefficient of chemical swelling. Without loss of generality, one can then use $\hat{a}_{\alpha\beta} = J_{\text{in}} A_{\alpha\beta}$ as discussed in Sec. 3.3.

ii. Chemical bending: An example for concentration induced curvature increase is the isotopic bending model (52) with the linear curvature increase

$$\bar{\kappa}_{\text{in}} = 1 + \alpha_\kappa (\phi - \phi_0), \quad (166)$$

where α_κ is a constant. This curvature increase could be caused by a one-sided swelling, e.g. due to the binding of molecules to one side of a flexible membrane (Sahu et al., 2017).

Another, less trivial, example is a curvature increase due to a concentration difference between top and bottom surface, i.e.

$$\bar{\kappa}_{\text{in}} = 1 + \alpha_\kappa (\phi_+ - \phi_-), \quad (167)$$

where ϕ_+ and ϕ_- denote the top and bottom concentrations of surface \mathcal{S} , respectively. These need to be defined in a suitable way, e.g. by using two separate PDEs of type (104) for the top and bottom surface.

iii. Surface mass diffusion: A simple surface diffusion model satisfying (149) is

$$j^\alpha = -M a^{\alpha\beta} \left(\frac{\mu}{T} \right)_{;\beta}, \quad (168)$$

where M is a constant. Choosing

$$\psi = \frac{c_\phi}{2} T \phi^2, \quad (169)$$

¹²w.r.t. stretch $\lambda_{\text{in}} = \sqrt{J_{\text{in}}}$

where c_ϕ is a constant, we find the chemical potential

$$\mu = c_\phi T \phi - \frac{1}{\rho J} \left(2\alpha_c \gamma_0 \lambda_{\text{in}} + 4\alpha_c \gamma_0^{\text{M}} \lambda_{\text{in}} \bar{\kappa}_{\text{in}} + 2\alpha_\kappa \gamma_0^{\text{M}} \lambda_{\text{in}}^2 \right), \quad (170)$$

due to (152), (50), (55), (165) and (166). Here $\gamma_0 := \sigma_0^{\alpha\beta} A_{\alpha\beta}/2$ and $\gamma_0^{\text{M}} := M_0^{\alpha\beta} B_{\alpha\beta}/2$ follow from the stress definitions in Eq. (123) and Sec. 5.2.1. For the special case that γ_0 , γ_0^{M} and T are constant across \mathcal{S} , we arrive at Fick's law

$$j^\alpha = -D a^{\alpha\beta} \phi_{;\beta}, \quad (171)$$

where $D = \tilde{c}_\phi M$, with $\tilde{c}_\phi = c_\phi - (2\alpha_c^2 \gamma_0 + 4\alpha_c^2 \gamma_0^{\text{M}} \bar{\kappa}_{\text{in}} + 8\alpha_c \alpha_\kappa \gamma_0^{\text{M}} \lambda_{\text{in}})/(T \rho J)$, is the surface diffusivity.

7.3.3 Mechanical membrane models

This section discusses mechanical material models for elastic, viscous and plastic membrane behavior, for which bending moments are neglected. In this case we have $N^{\alpha\beta} = \sigma^{\alpha\beta}$ according to (123).

i. Surface elasticity: An example for the elastic response is the potential

$$\hat{\Psi} = \frac{\Lambda}{4} (J_{\text{el}}^2 - 1 - 2 \ln J_{\text{el}}) + \frac{G}{2} (I_1^{\text{el}} - 2 - 2 \ln J_{\text{el}}), \quad (172)$$

which is adapted from the classical 3D Neo-Hookean material model (Sauer and Duong, 2017). The parameters Λ and G are material constants. From (172) follows the membrane stress

$$\sigma_{(\text{el})}^{\alpha\beta} = \frac{\Lambda}{2J_{\text{el}}} (J_{\text{el}}^2 - 1) a^{\alpha\beta} + \frac{G}{J_{\text{el}}} (\hat{a}^{\alpha\beta} - a^{\alpha\beta}), \quad (173)$$

according to (157), (82) and (84). The two terms in (172) do not properly split dilatational and deviatoric energies. Such a split is achieved by the alternative model

$$\hat{\Psi} = \frac{K}{4} (J_{\text{el}}^2 - 1 - 2 \ln J_{\text{el}}) + \frac{G}{2} \left(\frac{I_1^{\text{el}}}{J_{\text{el}}} - 2 \right), \quad (174)$$

which is adapted from Sauer and Duong (2017). The constants K and G denote the in-plane bulk and shear moduli. From (157) now follows the membrane stress

$$\sigma_{(\text{el})}^{\alpha\beta} = \frac{K}{2J_{\text{el}}} (J_{\text{el}}^2 - 1) a^{\alpha\beta} + \frac{G}{J_{\text{el}}^2} \left(\hat{a}^{\alpha\beta} - \frac{I_1^{\text{el}}}{2} a^{\alpha\beta} \right). \quad (175)$$

Here the first part is purely dilatational, while the second is purely deviatoric. Hence, the surface tension only depends on the first part, while the deviatoric stress only depends on the second part: From (108) and (109) follow the surface tension

$$\gamma = \frac{K}{2J_{\text{el}}} (J_{\text{el}}^2 - 1) \quad (176)$$

and the deviatoric stress

$$\sigma_{\text{dev}}^{\alpha\beta} = \frac{G}{J_{\text{el}}^2} \left(\hat{a}^{\alpha\beta} - \frac{I_1^{\text{el}}}{2} a^{\alpha\beta} \right). \quad (177)$$

A third elasticity example is the linear elastic membrane model

$$\hat{\Psi} = \frac{1}{2} \varepsilon_{\alpha\beta}^{\text{el}} \hat{c}^{\alpha\beta\gamma\delta} \varepsilon_{\gamma\delta}^{\text{el}}, \quad (178)$$

with the material tangent

$$\hat{c}^{\alpha\beta\gamma\delta} := \Lambda \hat{a}^{\alpha\beta} \hat{a}^{\gamma\delta} + G (\hat{a}^{\alpha\gamma} \hat{a}^{\beta\delta} + \hat{a}^{\alpha\delta} \hat{a}^{\beta\gamma}) \quad (179)$$

based on the constants Λ and G . (178) is analogous to the 3D St.-Venant-Kirchhoff material, from which it can be derived¹³. From (158) now follows

$$\hat{\sigma}_{(\text{el})}^{\alpha\beta} = \hat{c}^{\alpha\beta\gamma\delta} \varepsilon_{\gamma\delta}^{\text{el}}, \quad (180)$$

which can be expanded into

$$\hat{\sigma}_{(\text{el})}^{\alpha\beta} = \frac{\Lambda}{2} (I_1^{\text{el}} - 2) \hat{a}^{\alpha\beta} + G (\hat{a}^{\alpha\gamma} a_{\gamma\delta} \hat{a}^{\beta\delta} - \hat{a}^{\alpha\beta}). \quad (181)$$

ii. Surface viscosity: A simple shear viscosity model satisfying (149) is

$$\hat{\sigma}_{(\text{in})}^{\alpha\beta} = -\eta \dot{\hat{a}}^{\alpha\beta}, \quad (182)$$

where the material constant $\eta \geq 0$ denotes the in-plane shear viscosity.¹⁴ It is noted, that model (182) is not purely deviatoric, since it generally leads to non-zero surface tension ($\gamma = \frac{1}{2} \sigma^{\alpha\beta} a_{\alpha\beta} \neq 0$). Another simple viscosity model satisfying (149) is

$$\hat{\sigma}_{(\text{in})}^{\alpha\beta} = \lambda \dot{J}_{\text{in}} \hat{a}^{\alpha\beta}, \quad (183)$$

where the material constant $\lambda \geq 0$ denotes the in-plane bulk viscosity.¹⁵ It is noted, that model (183) is not purely dilatational, since it generally leads to non-zero shear stresses.

If there is no elastic deformation, $\hat{a}_{\alpha\beta} = a_{\alpha\beta}$. If there is elastic deformation, $\hat{a}_{\alpha\beta}$ has to be determined from an evolution law. This depends on the rheological model considered. For a

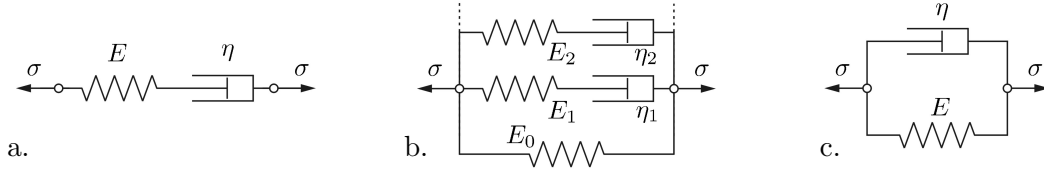


Figure 2: Surface rheology: a. viscoelastic Maxwell fluid; b. generalized viscoelastic solid; c. viscoelastic Kelvin solid. Even though these are 1D models, they can be used in 2D and 3D, e.g. by applying them to dilatation and shear. E then plays the role of bulk and shear modulus.

Maxwell element, see Fig. 2a, the evolution law for $\hat{a}^{\alpha\beta}$ follows from

$$\sigma_{(\text{el})}^{\alpha\beta}(\hat{a}^{\gamma\delta}) = \sigma_{(\text{in})}^{\alpha\beta}(\hat{a}^{\gamma\delta}, \dot{\hat{a}}^{\gamma\delta}), \quad (184)$$

which is a nonlinear ODE that can be solved locally using numerical methods (e.g. implicit Euler). For example, for models (173) and (182), the evolution law is

$$\dot{\hat{a}}^{\alpha\beta} = \frac{\Lambda}{2\eta} (1 - J_{\text{el}}^2) a^{\alpha\beta} + \frac{G}{\eta} (a^{\alpha\beta} - \hat{a}^{\alpha\beta}), \quad (185)$$

¹³A 3D energy density needs to be multiplied by the shell thickness in order to obtain the membrane energy density $\hat{\Psi}$.

¹⁴Proof: Using $\dot{\hat{a}}^{\alpha\beta} = -\hat{a}^{\alpha\gamma} \dot{\hat{a}}_{\gamma\delta} \hat{a}^{\beta\delta}$ and $2\hat{\mathbf{D}} := \dot{\hat{a}}_{\alpha\beta} \hat{\mathbf{a}}^\alpha \otimes \hat{\mathbf{a}}^\beta$ gives $\sigma_{(\text{in})}^{\alpha\beta} \dot{\varepsilon}_{\alpha\beta}^{\text{in}} = 2\eta \hat{\mathbf{D}} : \hat{\mathbf{D}} / J_{\text{el}} \geq 0$ for $\eta \geq 0$.

¹⁵Proof: From (81) follows $\sigma_{(\text{in})}^{\alpha\beta} \dot{\varepsilon}_{\alpha\beta}^{\text{in}} = 2\lambda \dot{J}_{\text{in}} / J \geq 0$ for $\lambda \geq 0$.

where J_{el} is a function of $\hat{a}^{\alpha\beta}$ according to (45). A second example is to use models (175) and (183) and consider only inelastic dilatation ($\hat{a}_{\alpha\beta} = J_{\text{in}} A_{\alpha\beta}$) according to Sec. 3.3. Contracting (184) with $a_{\alpha\beta}$ and using the relations from Sec. 3.3 thus yields the evolution law

$$\dot{J}_{\text{in}} = \frac{K}{\lambda} \frac{J}{I_1} \left(\frac{J}{J_{\text{in}}} - \frac{J_{\text{in}}}{J} \right) \quad (186)$$

for J_{in} .

For a generalized viscoelastic solid, see Fig. 2b, evolution law (184) needs to be solved for $\hat{a}_M^{\alpha\beta}$ within each Maxwell element M . This defines the stress $\sigma_M^{\alpha\beta}$ in each Maxwell element. The total stress is then the sum of the stresses in all elements, i.e.

$$\sigma^{\alpha\beta} = \sigma_{\text{el}0}^{\alpha\beta}(a^{\gamma\delta}) + \sum_{M=1} \sigma_M^{\alpha\beta}(\hat{a}_M^{\gamma\delta}). \quad (187)$$

This model contains the special cases of a single Maxwell element – for $M = 1$ and $\sigma_{\text{el}0}^{\alpha\beta} = 0$ – and the Kelvin model – for $M = 1$ and $\hat{a}^{\alpha\beta} = a^{\alpha\beta}$ (see Fig. 2c).

Remark 7: Apart of (182) and (183), also the slightly different choices $\sigma_{(\text{in})}^{\alpha\beta} = -\eta \dot{\hat{a}}^{\alpha\beta}$ and $\sigma_{(\text{in})}^{\alpha\beta} = \lambda \dot{J}_{\text{in}} \hat{a}^{\alpha\beta}$ are consistent with the second law.

iii. Surface constraints: Constraints are important for various applications. A popular example is incompressibility, which is discussed in the following.

Elastic incompressibility implies $J_{\text{el}} \equiv 1$. This conditions leads to an extra stress that can for example be captured by the Lagrange multiplier method. According to this, the stress follows from the potential

$$\hat{\Psi} = q (J_{\text{el}} - 1), \quad (188)$$

where q is the corresponding Lagrange multiplier. The constraint stress, according to (157) and (82), thus is

$$\sigma_{(\text{el})}^{\alpha\beta} = q a^{\alpha\beta}, \quad (189)$$

i.e. it is dilatational. The Lagrange multiplier q is an additional unknown that needs to be solved for. It can be avoided by considering the penalty regularization

$$\hat{\Psi} = \frac{K}{2} (J_{\text{el}} - 1)^2, \quad (190)$$

where the in-plane bulk modulus K is set to a very large value to ensure $J_{\text{el}} \approx 1$. From (157) and (82) now follows

$$\sigma_{(\text{el})}^{\alpha\beta} = K (J_{\text{el}} - 1) a^{\alpha\beta}. \quad (191)$$

Inelastic incompressibility implies $J_{\text{in}} \equiv 1$, i.e. $\dot{J}_{\text{in}} = 0$. According to (81) this leads to the constraint

$$\dot{\hat{a}}^{\alpha\beta} \hat{a}_{\alpha\beta} = 0 \quad (192)$$

on the internal variable $\hat{a}_{\alpha\beta}$. This is a scalar equation, and so two more equations are needed in order to determine $\hat{a}_{\alpha\beta}$. We can find those by contracting the evolution law with $\hat{a}_{\alpha\beta}$ and $a_{\alpha\beta}$. For evolution law (185) we thus find

$$0 = \Lambda (1 - J_{\text{el}}^2) + G (2 - 4/I_{1-}^{\text{el}}) \quad (193)$$

and

$$\dot{\hat{a}}^{\alpha\beta} a_{\alpha\beta} = \frac{\Lambda}{\eta} (1 - J_{\text{el}}^2) + \frac{G}{\eta} (2 - I_1^{\text{el}}). \quad (194)$$

Eqs. (192)-(194) can then be solved for $\hat{a}_{\alpha\beta}$.

iv. Surface plasticity: Plastic behavior can be characterized by the yield surface $f_y = f_y(\sigma^{\alpha\beta}) = 0$ that satisfies $\dot{f}_y = 0$ during plastic flow. Hence,

$$\frac{\partial f_y}{\partial \sigma^{\alpha\beta}} \dot{\sigma}^{\alpha\beta} = 0. \quad (195)$$

A common approach to determine an evolution equation for $\hat{a}_{\alpha\beta}$ from this is to use the principle of maximum dissipation. This assumes that for a given inelastic strain rate $\dot{\varepsilon}_{\alpha\beta}^{\text{in}}$, the true stress is the one that maximizes the dissipation $\sigma^{\alpha\beta} \dot{\varepsilon}_{\alpha\beta}^{\text{in}}$ among all possible stress states. This implies

$$\dot{\sigma}^{\alpha\beta} \dot{\varepsilon}_{\alpha\beta}^{\text{in}} = 0. \quad (196)$$

Together, Eqs. (195) and (196) imply that

$$\dot{\varepsilon}_{\alpha\beta}^{\text{in}} = \lambda \frac{\partial f_y}{\partial \sigma^{\alpha\beta}}, \quad (197)$$

which is the evolution law for $\hat{a}_{\alpha\beta}$. The scalar λ follows from the condition $\dot{f}_y = 0$.

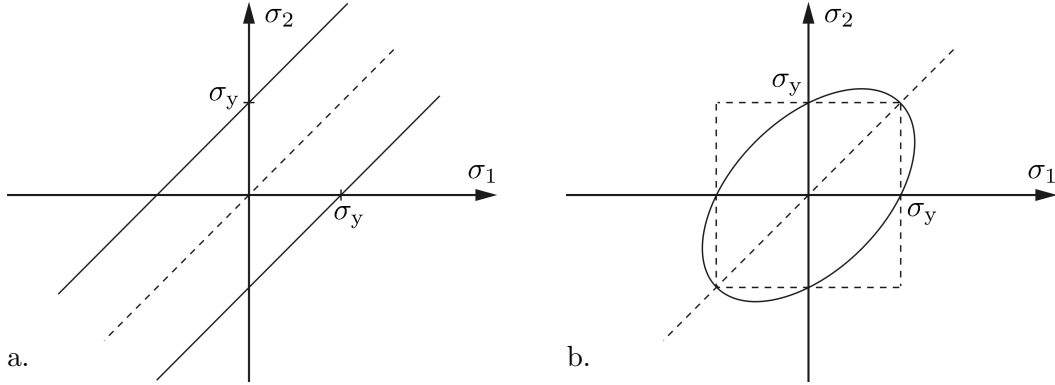


Figure 3: Surface plasticity: Yield surface $f_y = 0$ in principal stress space for a. 2D von Mises plasticity and b. 3D von Mises plasticity.

An example (that is a 2D version of von Mises plasticity¹⁶, see Fig. 3a) is

$$f_y := \hat{s} - \frac{\sqrt{2}}{2} \sigma_y, \quad (198)$$

where the material constant σ_y denotes the yield stress, and

$$\hat{s} := \sqrt{\hat{\sigma}_{\text{dev}}^{\alpha\beta} \hat{\sigma}_{\text{dev}}^{\alpha\beta}} \quad (199)$$

defines the 2D von Mises stress from the deviatoric stress

$$\hat{\sigma}_{\text{dev}}^{\alpha\beta} := \hat{\sigma}^{\alpha\beta} - \hat{\gamma} \hat{a}^{\alpha\beta}, \quad \hat{\sigma}_{\text{dev}}^{\alpha\beta} := \hat{a}_{\alpha\gamma} \hat{\sigma}^{\gamma\delta} \hat{a}_{\delta\beta} \quad (200)$$

and the surface tension

$$\hat{\gamma} := \frac{1}{2} \hat{\sigma}^{\alpha\beta} \hat{a}_{\alpha\beta}, \quad (201)$$

¹⁶Another possibility is to use the classical 3D von Mises plasticity model together with the plane stress assumption. In this case $f_y := \|\hat{\sigma}_{\text{dev}}\| - \sqrt{2/3} \sigma_y$, where $\hat{\sigma}_{\text{dev}}$ is the full 3D stress deviator. See Fig. 3b.

similar to definitions (108) and (110). From

$$\frac{\partial \dots}{\partial \sigma^{\alpha\beta}} = J_{\text{el}} \frac{\partial \dots}{\partial \hat{\sigma}^{\alpha\beta}} \quad (202)$$

and

$$\hat{\sigma}_{\alpha\beta}^{\text{dev}} \hat{a}^{\alpha\beta} = \hat{\sigma}_{\text{dev}}^{\alpha\beta} \hat{a}_{\alpha\beta} = 0, \quad (203)$$

then follows

$$\frac{\partial f_y}{\partial \sigma^{\alpha\beta}} = J_{\text{el}} \frac{\hat{\sigma}_{\alpha\beta}^{\text{dev}}}{\hat{s}}, \quad (204)$$

such that

$$\varepsilon_{\alpha\beta}^{\text{in}} = \hat{\lambda} \frac{\hat{\sigma}_{\alpha\beta}^{\text{dev}}}{\hat{s}}, \quad (205)$$

with $\hat{\lambda} := J_{\text{el}} \lambda$, and

$$\sigma^{\alpha\beta} \varepsilon_{\alpha\beta}^{\text{in}} = \lambda \hat{s}. \quad (206)$$

Eq. (149) is thus satisfied for $\lambda \geq 0$. From (74), (203) and (205) follows that $\dot{\hat{a}}_{\alpha\beta} \hat{a}^{\alpha\beta} = 0$, i.e. plasticity model (205) is inelastically incompressible.

7.3.4 Mechanical bending models

i. Bending elasticity: An example for a linear bending model is

$$\hat{\Psi} = \frac{1}{2} \kappa_{\alpha\beta}^{\text{el}} \hat{f}^{\alpha\beta\gamma\delta} \kappa_{\gamma\delta}^{\text{el}}, \quad (207)$$

where $\hat{f}^{\alpha\beta\gamma\delta}$ are the components of a constant material tensor. For shells made of a homogenous material, those are given by

$$\hat{f}^{\alpha\beta\gamma\delta} = \frac{h_0^2}{12} \hat{c}^{\alpha\beta\gamma\delta}, \quad (208)$$

where h_0 is the initial shell thickness and $\hat{c}^{\alpha\beta\gamma\delta}$ is given by (179). This bending model can be derived from the 3D St.-Venant-Kirchhoff material model via thickness integration, e.g. see Duong et al. (2017) for the purely elastic case. From (158) and (207) follows

$$\hat{M}_{(\text{el})}^{\alpha\beta} = \hat{f}^{\alpha\beta\gamma\delta} \kappa_{\gamma\delta}^{\text{el}}. \quad (209)$$

An example for a nonlinear bending model is

$$\hat{\Psi} = J_{\text{el}} \left(k_{\text{m}} (H - \hat{H})^2 + \frac{k_{\text{g}}}{2} (\kappa - \hat{\kappa})^2 \right), \quad (210)$$

where k_{m} and k_{g} are material constants. The model is an adaption and modification of the bending model by Helfrich (1973). It produces the bending moment components

$$M_{(\text{el})}^{\alpha\beta} = k_{\text{m}} (H - \hat{H}) a^{\alpha\beta} + k_{\text{g}} (\kappa - \hat{\kappa}) \tilde{b}^{\alpha\beta} \quad (211)$$

and stress components

$$\sigma_{(\text{el})}^{\alpha\beta} = \frac{\hat{\Psi}}{J_{\text{el}}} a^{\alpha\beta} - 2k_{\text{m}} (H - \hat{H}) b^{\alpha\beta} - 2k_{\text{g}} \kappa (\kappa - \hat{\kappa}) a^{\alpha\beta}, \quad (212)$$

due to (92)-(95). Here, $\tilde{b}^{\alpha\beta} := 2H a^{\alpha\beta} - b^{\alpha\beta}$.

ii. Bending viscosity: An analogous model to (182) is the bending viscosity model

$$\hat{M}_{\alpha\beta}^{(\text{in})} = \eta_b \dot{\hat{b}}_{\alpha\beta}, \quad (213)$$

since it satisfies (149) for an analogous proof as for (182). Setting this equal to $\hat{M}_{\alpha\beta}^{(\text{el})}$ (i.e. assuming a Maxwell model) then yields the evolution law for $\hat{b}_{\alpha\beta}$. For example taking (209) with $\hat{f}^{\alpha\beta\gamma\delta} = f_0 (\hat{a}^{\alpha\gamma}\hat{a}^{\beta\delta} + \hat{a}^{\alpha\delta}\hat{a}^{\beta\gamma})/2$ yields the simple linear evolution law

$$\dot{\hat{b}}_{\alpha\beta} = \frac{f_0}{\eta_b} (b_{\alpha\beta} - \hat{b}_{\alpha\beta}). \quad (214)$$

iii. Bending plasticity: Accounting for bending, the yield surface from Sec. 7.3.3.iv needs to be extended to $f_y(\sigma^{\alpha\beta}, M^{\alpha\beta})$, such that during plastic flow

$$\frac{\partial f_y}{\partial \sigma^{\alpha\beta}} \dot{\sigma}^{\alpha\beta} + \frac{\partial f_y}{\partial M^{\alpha\beta}} \dot{M}^{\alpha\beta} = 0. \quad (215)$$

Invoking again the principle of maximum dissipation, which assumes that for given inelastic strain rates $\dot{\varepsilon}_{\alpha\beta}^{\text{in}}$ and $\dot{\kappa}_{\alpha\beta}^{\text{in}}$, the true stress and bending moment components are those that maximize the dissipation $\sigma^{\alpha\beta}\dot{\varepsilon}_{\alpha\beta}^{\text{in}} + M^{\alpha\beta}\dot{\kappa}_{\alpha\beta}^{\text{in}}$ among all possible stress states, we find

$$\dot{\sigma}^{\alpha\beta}\dot{\varepsilon}_{\alpha\beta}^{\text{in}} + \dot{M}^{\alpha\beta}\dot{\kappa}_{\alpha\beta}^{\text{in}} = 0. \quad (216)$$

Multiplying Eq. (215) by λ and subtracting it from (216) then gives

$$\left(\dot{\varepsilon}_{\alpha\beta}^{\text{in}} - \lambda \frac{\partial f_y}{\partial \sigma^{\alpha\beta}} \right) \dot{\sigma}^{\alpha\beta} + \left(\dot{\kappa}_{\alpha\beta}^{\text{in}} - \lambda \frac{\partial f_y}{\partial M^{\alpha\beta}} \right) \dot{M}^{\alpha\beta} = 0, \quad (217)$$

Since this is true for all $\dot{\sigma}^{\alpha\beta}$ and $\dot{M}^{\alpha\beta}$ we find the flow rules (197) and

$$\dot{\kappa}_{\alpha\beta}^{\text{in}} = \lambda \frac{\partial f_y}{\partial M^{\alpha\beta}}, \quad (218)$$

which are the evolution laws for $\hat{a}_{\alpha\beta}$ and $\hat{b}_{\alpha\beta}$. The scalar λ again follows from the condition $\dot{f}_y = 0$.

As an example we consider the simple extension of (198),

$$f_y := \frac{\hat{s}}{\sigma_y} + \frac{\hat{s}_M}{M_y} - \frac{\sqrt{2}}{2}, \quad (219)$$

where the material constant M_y denotes the yield limit for bending, and

$$\hat{s}_M := \sqrt{\hat{M}_{\text{dev}}^{\alpha\beta} \hat{M}_{\alpha\beta}^{\text{dev}}} \quad (220)$$

with

$$\hat{M}_{\text{dev}}^{\alpha\beta} := \hat{M}^{\alpha\beta} - \hat{\gamma}_M \hat{a}^{\alpha\beta}, \quad \hat{M}_{\alpha\beta}^{\text{dev}} := \hat{a}_{\alpha\gamma} \hat{M}_{\text{dev}}^{\gamma\delta} \hat{a}_{\delta\beta} \quad (221)$$

and

$$\hat{\gamma}_M := \frac{1}{2} \hat{M}^{\alpha\beta} \hat{a}_{\alpha\beta}, \quad (222)$$

is defined analogous to (199)-(201). Due to this analogy, the flow rule for $\dot{\kappa}_{\alpha\beta}^{\text{in}}$ follows in analogy to (205), which is still valid here, as

$$\dot{\kappa}_{\alpha\beta}^{\text{in}} = \hat{\lambda} \frac{\hat{M}_{\alpha\beta}^{\text{dev}}}{\hat{s}_M}, \quad (223)$$

which also satisfies Eq. (149) for $\lambda \geq 0$.

The elasto-plasticity model described by the constitutive equations in (157), (197) and (218) is equivalent to the model of Simo and Kennedy (1992). However, in Simo and Kennedy (1992), (157) is written in terms of $\Phi = \rho_0 \psi$, the Helmholtz free energy per unit reference area (in the case of $h = 0$). Also, Simo and Kennedy (1992), consider an alternative model to (219) that is based on Shapiro (1961).

7.3.5 Thermal models

i. Thermal energy: Considering

$$\hat{\Psi} = C_H \left[(T - T_0) - T \ln \frac{T}{T_0} \right], \quad (224)$$

where C_H is a material constant and T_0 is a constant reference temperature (Holzapfel, 2000), gives the specific entropy

$$s = \frac{C_H}{\hat{\rho}} \ln \frac{T}{T_0}, \quad (225)$$

due to (149) and (156). This energy does not generate stresses. Those only appear in response to mechanical deformations. Due to (224), the stored energy (per intermediate area) is $\hat{\rho} u = \hat{\rho}(\psi + Ts) = C_H(T - T_0)$.

ii. Surface heat conduction: A simple surface conductivity model satisfying (149) is Fourier's law

$$q^\alpha = -k a^{\alpha\beta} T_{;\beta}, \quad (226)$$

where the constant k is the surface heat conductivity. Model (226) is analogous to Fick's law (171).

iii. Thermal surface expansion: A simple linear model for isotropic thermal expansion (analogous to chemical swelling) is

$$J_{\text{in}} = \lambda_{\text{in}}^2, \quad \lambda_{\text{in}} = 1 + \alpha_T (T - T_0), \quad (227)$$

where the material constant α_T denotes the coefficient of thermal expansion. Without loss of generality, one can then use $\hat{a}_{\alpha\beta} = J_{\text{in}} A_{\alpha\beta}$ as discussed in Sec. 3.3. Model (227) leads to an additional entropy contribution due to (152), analogous to the contribution in μ seen in (170).

iv. Thermal bending: An example for temperature induced curvature increase is the isotropic bending model (52) with the linear curvature increase

$$\bar{\kappa}_{\text{in}} = 1 + \alpha_\kappa (T - T_0), \quad (228)$$

analogous to (166). Here α_κ is a material constant. This curvature increase could be caused by a one-sided thermal expansion. Analogous to (167), one can also consider the model

$$\bar{\kappa}_{\text{in}} = 1 + \alpha_\kappa (T_+ - T_-), \quad (229)$$

where T_+ and T_- denote the top and bottom temperatures of surface \mathcal{S} , respectively. Those need to be defined in a suitable way, e.g. by using two separate PDEs of type (129) for the top and bottom surface. Note that, models (228) and (229) lead to an additional entropy contribution due to (152), analogous to the contribution in μ seen in (170).

8 Conclusion

This work presents a general nonlinear shell theory for coupled elastic and inelastic deformations, accounting for growth, swelling, plasticity, viscosity and thermal expansion. The formulation is derived from the balance laws of mass, momentum, energy and entropy using a multiplicative split of the surface deformation gradient into elastic and inelastic contributions. The general constitutive equations of this coupling are derived and illustrated by several examples. Those

generally require the derivatives of various kinematical quantities w.r.t. the elastic and inelastic deformations.

Although the present formulation is purely theoretical, it is suitable for computational analysis, for example within the finite element method. There has been important recent progress on rotation-free finite elements (FE) in the framework of isogeometric analysis (Kiendl et al., 2009). Such FE formulations allow for a very accurate yet efficient surface description that is particularly beneficial for an accurate representation of curvatures. It can thus be expected that isogeometric shell FE formulations for coupled inelastic and elastic deformations would be very beneficial. So far, it seems that only elasto-plasticity and isotropic thermoelasticity have been analyzed with multiplicatively split isogeometric shell FE (Ambati et al., 2018; Vu-Bac et al., 2019). But the authors are currently applying the present theory to extend the hyperelastic graphene FE model of Ghaffari and Sauer (2018) to anisotropic thermoelasticity (Ghaffari and Sauer, 2019), and to study the growth of fluid films using the FE model of Sauer (2014) and Roohbakhshan and Sauer (2019).

Acknowledgements

The authors are grateful to the German Research Foundation (DFG) for funding this research under grant GSC 111. The authors also like to thank Farshad Roohbakhshan for feedback on the manuscript.

References

- Ahmad, S., Irons, B. M., and Zienkiewicz, O. C. (1970). Analysis of thick and thin shell structures by curved finite elements. *Int. J. Numer. Meth. Engng.*, **2**(3):419–451.
- Altenbach, H. and Eremeyev, V. (2015). On the constitutive equations of viscoelastic micropolar plates and shells of differential type. *Math. Mech. Complex Syst.*, **3**(3):273–283.
- Ambati, M., Kiendl, J., and De Lorenzis, L. (2018). Isogeometric Kirchhoff-Love shell formulation for elasto-plasticity. *Comput. Methods Appl. Mech. Engrg.*, **340**:320–339.
- Başar, Y. and Weichert, D. (1991). A finite-rotation theory for elastic-plastic shells under consideration of shear deformations. *ZAMM*, **71**(10):379–389.
- Betsch, P. and Stein, E. (1999). Numerical implementation of multiplicative elasto-plasticity into assumed strain elements with application to shells at large strains. *Comput. Methods Appl. Mech. Eng.*, **179**(3):215–245.
- Bilby, B. A., Lardner, L. R. T., and Stroh, A. N. (1957). Continuous distributions of dislocations and the theory of plasticity. In *Actes du IXe congrès international de mécanique appliquée (Bruxelles, 1956)*, volume **8**, pages 35–44. Université libre de Bruxelles.
- Coleman, B. D. and Noll, W. (1964). The thermodynamics of elastic materials with heat conduction and viscosity. *Arch. Ration. Mech. Anal.*, **13**:167–178.
- de Groot, S. R. and Mazur, P. (1984). *Non-equilibrium thermodynamics*. Dover.
- Dervaux, J., Ciarletta, P., and Amar, M. B. (2009). Morphogenesis of thin hyperelastic plates: A constitutive theory of biological growth in the Föppl-von Kármán limit. *J. Mech. Phys. Solids*, **57**(3):458–471.

- Dörr, D., Schirmaier, F. J., Henning, F., and Kärger, L. (2017). A viscoelastic approach for modeling bending behavior in finite element forming simulation of continuously fiber reinforced composites. *Compos. Part A: Appl. Sci. Manuf.*, **94**:113–123.
- Dujc, J. and Brank, B. (2012). Stress resultant plasticity for shells revisited. *Comput. Methods Appl. Mech. Engrg.*, 247-248:146–165.
- Duong, T. X., Roohbakhshan, F., and Sauer, R. A. (2017). A new rotation-free isogeometric thin shell formulation and a corresponding continuity constraint for patch boundaries. *Comput. Methods Appl. Mech. Engrg.*, **316**:43–83.
- Eberlein, R. and Wriggers, P. (1999). Finite element concepts for finite elastoplastic strains and isotropic stress response in shells: theoretical and computational analysis. *Comput. Methods Appl. Mech. Engrg.*, **171**(3):243–279.
- Eckart, C. (1948). The thermodynamics of irreversible processes. IV. the theory of elasticity and anelasticity. *Phys. Rev.*, **73**:373–382.
- Flory, P. J. (1950). Statistical mechanics of swelling of network structures. *J. Chem. Phys.*, **18**(1):108–111.
- Ghaffari, R., Duong, T. X., and Sauer, R. A. (2017). A new shell formulation for graphene structures based on existing ab-initio data. *Int. J. Solids Struct.*, **135**:37–60.
- Ghaffari, R. and Sauer, R. A. (2018). A new efficient hyperelastic finite element model for graphene and its application to carbon nanotubes and nanocones. *Finite Elem. Anal. Des.*, **146**:42–61.
- Ghaffari, R. and Sauer, R. A. (2019). Nonlinear thermomechanical formulations for anisotropic volume and surface continua. <https://arxiv.org>, 1901.00917.
- Green, A. E. and Naghdi, P. M. (1979). On thermal effects in the theory of shells. *Proc. Royal Soc. A*, **365**(1721):161–190.
- Green, A. E., Naghdi, P. M., and Osborn, R. (1968). Theory of an elastic-plastic cosserat surface. *Int. J. Solids Struct.*, **4**(9):907–927.
- Gupta, A., Steigmann, D. J., and Stölken, J. (2007). On the evolution of plasticity and incompatibility. *Math. Mech. Solids*, **12**:583–610.
- Helfrich, W. (1973). Elastic properties of lipid bilayers: Theory and possible experiments. *Z. Naturforsch.*, **28c**:693–703.
- Holzappel, G. A. (2000). *Nonlinear Solid Mechanics: A Continuum Approach for Engineering*. Wiley, Hoboken.
- Javili, A., McBride, A., Steinmann, P., and Reddy, B. D. (2014). A unified computational framework for bulk and surface elasticity theory: A curvilinear-coordinate-based finite element methodology. *Comput. Mech.*, **54**(3):745–762.
- Kar, V. R. and Panda, S. K. (2016). Nonlinear thermomechanical deformation behaviour of P-FGM shallow spherical shell panel. *Chin. J. Aeronaut.*, **29**(1):173–183.
- Kiendl, J., Bletzinger, K.-U., Linhard, J., and Wüchner, R. (2009). Isogeometric shell analysis with Kirchhoff-Love elements. *Comput. Methods Appl. Mech. Engrg.*, **198**:3902–3914.

- Kondaurov, V. I. and Nikitin, L. V. (1987). Finite strains of viscoelastic muscle tissue. *J. Appl. Math. Mech.*, **51**(3):346–353.
- Kondo, K. (1949). A proposal of a new theory concerning the yielding of materials based on Riemannian geometry, I. *J. Soc. Appl. Mech. Jpn.*, **2**(11):123–128.
- Kreyszig, E. (1991). *Differential Geometry*. Dover.
- Kröner, E. (1959). Allgemeine Kontinuumstheorie der Versetzungen und Eigenspannungen. *Arch. Ration. Mech. Anal.*, **4**(1):273.
- Li, F. (2012). A justification of two-dimensional nonlinear viscoelastic shells model. *Abstr. Appl. Anal.*, **2012**:24.
- Liang, H. and Mahadevan, L. (2011). Growth, geometry, and mechanics of a blooming lily. *Proc. Natl. Acad. Sci.*, **108**(14):5516–5521.
- Libai, A. and Simmonds, J. G. (1998). *The Nonlinear Theory of Elastic Shells*. Cambridge University Press, Cambridge, 2nd edition.
- Lubarda, V. A. (2004). Constitutive theories based on the multiplicative decomposition of deformation gradient: Thermoelasticity, elastoplasticity, and biomechanics. *Appl. Mech. Rev.*, **57**(2):95–108.
- Lubarda, V. A. (2011). Rate-type elasticity and viscoelasticity of an erythrocyte membrane. *J. Mech. Mater. Struct.*, **6**(1):361–376.
- Lucantonio, A., Tomassetti, G., and DeSimone, A. (2017). Large-strain poroelastic plate theory for polymer gels with applications to swelling-induced morphing of composite plates. *Compos. Part B: Eng.*, **115**:330–340.
- Lychev, S. (2014). Equilibrium equations for transversely accreted shells. *ZAMM*, **94**(1-2):118–129.
- Miehe, C. (1998). A theoretical and computational model for isotropic elastoplastic stress analysis in shells at large strains. *Comput. Methods Appl. Mech. Eng.*, **155**(3):193–233.
- Naghdi, P. M. (1972). Theory of plates and shells. In Truesdell, C., editor, *Handbuch der Physik*, pages 425–640, Berlin. Springer.
- Naghdi, P. M. (1982). Finite deformation of elastic rods and shells. In Carlson, D. E. and Shields, R. T., editors, *Proceedings of the IUTAM Symposium on Finite Elasticity*, pages 47–103, The Hague. Martinus Nijhoff Publishers.
- Neff, P. (2005). A geometrically exact viscoplastic membrane-shell with viscoelastic transverse shear resistance avoiding degeneracy in the thin-shell limit. *ZAMP*, **56**(1):148–182.
- Papastavrou, A., Steinmann, P., and Kuhl, E. (2013). On the mechanics of continua with boundary energies and growing surfaces. *J. Mech. Phys. Solids*, **61**(6):1446–1463.
- Parisich, H. (1978). Geometrical nonlinear analysis of shells. *Comput. Methods Appl. Mech. Eng.*, **14**(2):159–178.
- Pietraszkiewicz, W. (1989). Geometrically nonlinear theories of thin elastic shells. *Adv. Mech.*, **12**(1):51–130.

- Prigogine, I. (1961). *Introduction to thermodynamics of irreversible processes*. Interscience Publishers.
- Rausch, M. K. and Kuhl, E. (2014). On the mechanics of growing thin biological membranes. *J. Mech. Phys. Solids*, **63**:128–140.
- Reddy, J. N. and Chin, C. D. (1998). Thermomechanical analysis of functionally graded cylinders and plates. *J. Therm. Stresses*, **21**(6):593–626.
- Reina, C., Djodom, L. F., Ortiz, M., and Conti, S. (2018). Kinematics of elasto-plasticity: Validity and limits of applicability of $\mathbf{F} = \mathbf{F}^e \mathbf{F}^p$ for general three-dimensional deformations. *J. Mech. Phys. Solids*, **121**:99–113.
- Roohbakhshan, F. and Sauer, R. A. (2016). Isogeometric nonlinear shell elements for thin laminated composites based on analytical thickness integration. *J. Micromech. Mol. Phys.*, **1**(3-4):1640010.
- Roohbakhshan, F. and Sauer, R. A. (2017). Efficient isogeometric thin shell formulations for soft biological materials. *Biomech. Model. Mechanobiol.*, **16**(5):1569–1597.
- Roohbakhshan, F. and Sauer, R. A. (2019). A finite membrane element formulation for surfactants. *Colloids Surf. A: Physicochem. Eng. Aspects*, **566**:84–103.
- Roychowdhury, A. and Gupta, A. (2018). On structured surfaces with defects: Geometry, strain incompatibility, stress field, and natural shapes. *J. Elast.*, **131**:239–276.
- Sahu, A., Sauer, R. A., and Mandadapu, K. K. (2017). Irreversible thermodynamics of curved lipid membranes. *Phys. Rev. E*, **96**:042409.
- Sauer, R. A. (2014). Stabilized finite element formulations for liquid membranes and their application to droplet contact. *Int. J. Numer. Meth. Fluids*, **75**(7):519–545.
- Sauer, R. A. (2018). On the computational modeling of lipid bilayers using thin-shell theory. In Steigmann, D., editor, *CISM Advanced School ‘On the role of mechanics in the study of lipid bilayers’*, pages 221–286. Springer.
- Sauer, R. A. and Duong, T. X. (2017). On the theoretical foundations of solid and liquid shells. *Math. Mech. Solids*, **22**(3):343–371.
- Sauer, R. A., Duong, T. X., Mandadapu, K. K., and Steigmann, D. J. (2017). A stabilized finite element formulation for liquid shells and its application to lipid bilayers. *J. Comput. Phys.*, **330**:436–466.
- Sawczuk, A. (1982). On plastic shell theories at large strains and displacements. *Int. J. Mech. Sci.*, **24**(4):231–244.
- Sedov, L. (1966). *Foundations of the non-linear mechanics of continua*. Pergamon Press, Oxford.
- Shapiro, G. S. (1961). On yield surfaces for ideally plastic shells. In *Problems of Continuum Mechanics*, pages 414–418. SIAM, Philadelphia.
- Sidoroff, F. (1974). Un modèle viscoélastique non linéaire avec configuration intermédiaire. *J. Méc.*, **13**(4):679–713.
- Simo, J. C. and Kennedy, J. G. (1992). On a stress resultant geometrically exact shell model. part v. nonlinear plasticity: formulation and integration algorithms. *Comput. Methods Appl. Mech. Engrg.*, **96**:133–171.

- Steigmann, D. J. (1999). On the relationship between the Cosserat and Kirchhoff-Love theories of elastic shells. *Math. Mech. Solids*, **4**:275–288.
- Steigmann, D. J. (2015). Mechanics of materially uniform thin films. *Math. Mech. Solids*, **20**(3):309–326.
- Stojanović, R., Djurić, S., and Vujošević, L. (1964). On finite thermal deformations. *Archiwum Mechaniki Stosowanej*, **1**(16):103108.
- Stumpf, H. and Schieck, B. (1994). Theory and analysis of shells undergoing finite elastic-plastic strains and rotations. *Acta Mech.*, **106**(1):1–21.
- Swain, D. and Gupta, A. (2018). Biological growth in bodies with incoherent interfaces. *Proc. R. Soc. A*, **474**:20170716.
- Takamizawa, K. and Hayashi, K. (1987). Strain energy density function and uniform strain hypothesis for arterial mechanics. *J. Biomech.*, **20**(1):7–17.
- van der Sman, R. G. M. (2015). Hyperelastic models for hydration of cellular tissue. *Soft Matter*, **11**:7579–7591.
- Vetter, R., Stoop, N., Jenni, T., Wittel, F. K., and Herrmann, H. J. (2013). Subdivision shell elements with anisotropic growth. *Int. J. Numer. Methods Eng.*, **95**(9):791–810.
- Vetter, R., Stoop, N., Wittel, F. K., and Herrmann, H. J. (2014). Simulating thin sheets: Buckling, wrinkling, folding and growth. *J. Phys.: Conf. Ser.*, **487**(1):012012.
- Vu-Bac, N., Duong, T. X., Lahmer, T., Areias, P., Sauer, R. A., Park, H. S., and Rabczuk, T. (2019). A NURBS-based inverse analysis of thermal expansion induced morphing of thin shells. *Comput. Methods Appl. Mech. Engrg.*, **350**:480–510.
- Vu-Bac, N., Duong, T. X., Lahmer, T., Zhuang, X., Sauer, R. A., Park, H. S., and Rabczuk, T. (2018). A NURBS-based inverse analysis for reconstruction of nonlinear deformations in thin shell structures. *Comput. Methods Appl. Mech. Engrg.*, **331**:427–455.
- Wang, J., Steigmann, D. J., Wang, F.-F., and Dai, H.-H. (2018). On a consistent finite-strain plate theory of growth. *J. Mech. Phys. Solids*, **111**:184–214.
- Zimmermann, C., Toshniwal, D., Landis, C. M., Hughes, T. J. R., Mandadapu, K. K., and Sauer, R. A. (2019). An isogeometric finite element formulation for phase fields on deforming surfaces. *Comput. Methods Appl. Mech. Engrg.*, **351**:441–477.